X 62 72183 Copy 537.

[redacted] NASA TM X-359

GPO PRICE $ ______

OTS PRICE(S) $ ______

Hard copy (HC) 3.00

Microfiche (MF) .75

TECHNICAL MEMORANDUM

X-359

NASA TM X-359

X-890 4-17-62

CASE FILE COPY

MANUAL-CONTROL SIMULATION STUDY OF A NONLIFTING VEHICLE DURING ORBIT, RETRO-ROCKET FIRING, AND REENTRY INTO THE EARTH'S ATMOSPHERE

By Roger M. Davidson, Donald C. Cheatham, and Jack T. Kaylor

Langley Research Center
Langley Field, Va.

DECLASSIFIED - EFFECTIVE 1-15-64
Authority: Memo Geo. Drobka NASA HQ.
Code ATSS-A Dtd. 3-12-64 Subj: Change
in Security Classification Marking.

[redacted]

N65-12802 (ACCESSION NUMBER) 62 (PAGES) TMX-359 (NASA CR OR TMX OR AD NUMBER) (THRU) 1 (CODE) 05 (CATEGORY)

FACILITY FORM 602

NATIONAL AERONAUTICS AND SPACE ADMINISTRATION

WASHINGTON September 1960

[redacted]

DECLASSIFIED

[redacted]

LV

NATIONAL AERONAUTICS AND SPACE ADMINISTRATION

TECHNICAL MEMORANDUM X-359

MANUAL-CONTROL SIMULATION STUDY OF A NONLIFTING VEHICLE DURING ORBIT, RETRO-ROCKET FIRING, AND REENTRY INTO THE EARTH'S ATMOSPHERE*

By Roger M. Davidson, Donald C. Cheatham, and Jack T. Kaylor

L 9 7 4

SUMMARY

12802

The six-degree-of-freedom equations of motion for a nonlifting reentry vehicle such as the Mercury capsule were solved by an analog computer. The pilot was used to close the control loop. A number of variations in instrument display, side-arm controller, and control-torque output variation with controller displacement were made. The conclusions reached as a result of both pilot opinion and data obtained were that a human pilot is capable of controlling the vehicle dynamics during orbital flight, retro-rocket firing (including large misalinement torques), and reentry. In general, orbital control was found easy and reentry control little more difficult. Control of the vehicle while firing the retro-rockets, with the associated large misalinement torques, was very difficult but possible.

author

INTRODUCTION

A study was made in order to determine the human-pilot control problems associated with the operation of a vehicle similar to the Project Mercury capsule. In this study the control of vehicle dynamics was considered during (a) orbit, (b) the firing of the retro-rockets, and (c) reentry into the atmosphere.

The study was conducted by utilizing an analog-computer solution of the equations of motion of the capsule together with a fixed cockpit in which a control system and instrument display were provided. A pilot interpreting the information of the instrument display and actuating the control system closed the loop between the computer and the cockpit and completed the simulation.

The equations of motion utilized provided a close simulation of the dynamics of the Mercury capsule. Several control systems and instrument

*Title, Unclassified.

[redacted]

displays, including some which were similar to early proposals for this capsule, were included in the study in order to gain a better understanding of some of the factors pertinent to the control problems. The control torque output with controller deflection was also varied, and included profiles similar to those tested in reference 1. Since it was desired to make a rather broad survey in a short period of time, only one pilot was used for most of the tests.

It is the purpose of this paper to describe the results of the study that has been performed and to discuss some of the more important aspects of the problems involved in manual control of such a vehicle. In addition, some results describing the use of a rate command system for control of a capsule are presented.

L
9
7
4

SYMBOLS

a_X component of acceleration along the X body axis, g units

d diameter of leading surface, ft

F_X,F_Y,F_Z aerodynamic forces along the X, Y, and Z body axes, respectively, ft/sec^2

g gravitational constant, 31.5 ft/sec^2

h altitude, ft

I_X,I_Y,I_Z moments of inertia about the X, Y, and Z body axes, respectively, slug-ft^2

K_1,K_2,K_3 fuel consumption constants, 0.00134/ft-sec, 0.00134/ft-sec, and 0.0022/ft-sec, respectively

k feedback gain

l_3,m_3,n_3 direction cosines of body-axis system referred to earth-stabilized axes

M mass of vehicle, slugs

M_X,M_Y,M_Z rolling, pitching, and yawing moments, respectively, ft-lb

p,q,r rolling, pitching, and yawing velocity, respectively, radians/sec

$\bar{q}$ — dynamic pressure, lb/sq ft

R — distance from center of the earth to mass center of vehicle, ft

S — reference area, sq ft

$T_{\delta_1}, T_{\delta_2}, T_{\delta_3}$ — roll, pitch, and yaw control torque, respectively, ft-lb

t — time, sec

u, v, w — velocity components along X, Y, and Z body axes, respectively, ft/sec

V — velocity, ft/sec

X, Y, Z — three orthogonal body axes of vehicle

α — angle of attack, deg

$\alpha^* = \alpha - \alpha_T$

α_T — trim angle of attack, deg

β — angle of sideslip, deg

$\beta^* = \beta - \beta_T$

β_T — trim angle of sideslip, deg

$\delta_1, \delta_2, \delta_3$ — roll, pitch, and yaw control deflections

ϵ — error signal

θ — pitch angle, deg

ρ — air density, slugs/cu ft

θ^*, ϕ^*, ψ^* — pitch, roll, and yaw peak-to-peak excursions during retro-rocket firing, respectively, deg

ϕ — roll angle, deg

ψ — yaw angle, deg

Subscripts:

α,β,δ denote partial derivatives of the variable with respect to subscript, except for T_{δ_1}, T_{δ_2}, and T_{δ_3}

max maximum

o initial

r denotes quantity is a result of retro-rocket firing L974

Dot over a quantity denotes differentiation with respect to time.

DESCRIPTION OF THE SIMULATION

Equations of Motion

Six degree-of-freedom equations written with respect to the principal body axes were utilized. In these equations a constant gravity field over a flat earth was assumed but terms representing components of centrifugal force were added to the force equations. This approach neglects the small angular rates necessary to maintain the body axes in a fixed relationship to the local horizon of a round earth; however, this angular rate is only of the order of 1/15 deg/sec. Such a low angular rate would have a negligible effect upon the control problem during firing of the retro-rocket and probably a minor effect on control during the orbit mode. The derivation of similar equations may be found in reference 2.

The force equations are as follows:

$$\dot{u} = vr - wq + l_3 g - F_X - l_3 \frac{V^2}{R} \tag{1}$$

$$\dot{v} = wp - ur + m_3 g - F_Y - m_3 \frac{V^2}{R} \tag{2}$$

$$\dot{w} = uq - vp + n_3 g - F_Z - n_3 \frac{V^2}{R} \tag{3}$$

where the terms

$$F_X = 1.55\bar{q}\frac{S}{M}\cos^2\alpha\,\cos^2\beta$$

$$F_Y = 0.35\beta\bar{q}\frac{S}{M}$$

and

$$F_Z = 0.35\alpha\bar{q}\frac{S}{M}$$

represent the aerodynamic forces along the X, Y, and Z body axes, respectively. Extrapolation of preliminary wind-tunnel data indicated little variation of force coefficients with Mach number above a Mach number of about 5 and therefore the force coefficients were assumed invariant with Mach number. During the orbit and retro-rocket-firing phases of the study the force equations were not used and therefore it was not necessary to include thrust terms in the equations.

The moment equations, which assume rigid-body dynamics, are as follows:

$$\dot{p} = \frac{I_Y - I_Z}{I_X}qr + \frac{M_{X\delta_1}(\delta_1)}{I_X} + \frac{M_{X,r}}{I_X} \tag{4}$$

$$\dot{q} = \frac{I_Z - I_X}{I_Y}rp + \frac{M_{Y_\alpha}\alpha^*}{I_Y} + \frac{M_{Y\delta_2}(\delta_2)}{I_Y} + \frac{M_{Y,r}}{I_Y} \tag{5}$$

$$\dot{r} = \frac{I_X - I_Y}{I_Z}pq + \frac{M_{Z_\beta}\beta^*}{I_Z} + \frac{M_{Z\delta_3}(\delta_3)}{I_Z} + \frac{M_{Z,r}}{I_Z} \tag{6}$$

The control moments were generated about all three axes by simulated reaction jets, and it was assumed that no cross-control moments were present. The nature of the controllers used and the profiles of control torque variation with deflection will be described in a later section entitled "Controllers." No aerodynamic damping terms were included in the moment equations because preliminary wind-tunnel test data showed a trend which indicated that at Mach numbers higher than 3 to 4 the damping coefficients would be small enough to neglect.

During the orbit and retro-rocket-firing phases of the study only the moment equations were used. The auxiliary equations used are as follows:

$$\alpha = \tan^{-1}\frac{w}{u} = \alpha^* + \alpha_T \tag{7}$$

$$\beta \approx \tan^{-1}\frac{v}{u} = \beta^* + \beta_T \qquad \text{(for small } \alpha) \tag{8}$$

$$\dot{h} = l_3 u + m_3 v + n_3 w \tag{9}$$

$$l_3 = -\sin\theta \tag{10}$$

$$m_3 = \cos\theta \sin\phi \tag{11}$$

$$n_3 = \cos\theta \cos\phi \tag{12}$$

$$\dot{\phi} = p + \dot{\psi}\sin\theta \tag{13}$$

$$\dot{\theta} = q\cos\phi - r\sin\phi \tag{14}$$

$$V^2 = u^2 + v^2 + w^2 \tag{15}$$

$$\dot{\psi} = \frac{r\cos\phi}{\cos\theta} + \frac{q\sin\phi}{\cos\theta} \tag{16}$$

The weight of fuel consumed is

$$K_1\int_0^t \left|T_{\delta_1}\right| dt + K_2\int_0^t \left|T_{\delta_2}\right| dt + K_3\int_0^t \left|T_{\delta_3}\right| dt \tag{17}$$

The dimensional and mass characteristics assumed for the capsule are as follows:

I_X, slug-ft^2	279
I_Y, slug-ft^2	442
I_Z, slug-ft^2	430
S, sq ft	34.8
d, ft	6.7
M, slugs	72.5

Cockpit

As a matter of expediency an existing cockpit mockup was used. This same cockpit with different display and control systems was used in the reentry-simulation study described in reference 3. The general layout of the cockpit may be seen in the photograph presented in figure 1, which shows the relative position of the pilot's seat with respect to the side-arm controller and instrument display panel.

Instrument Displays

Information displayed to the pilot during the different phases of the test program included pitch and roll attitude with respect to the local horizon, yaw attitude with respect to the initial direction of the velocity vector, information on angular rate about each of the body axes, and acceleration measured in g units along the X-axis of the capsule.

The display and the pilot's controller motions were consistent with the pilot's position facing rearward (see fig. 2). The signs of all pitching and rolling signals were therefore opposite in the cockpit to the corresponding signals in the computer. Three different display arrangements were included during the tests. They are described as follows:

<u>Display A</u>.- Figure 3 shows a photograph of display A. It consists of a centrally located instrument containing three needle indicators, each of which moves in translation, to give angular rate information for pitch, yaw, and roll motions. The pitch-rate information is provided by the needle that translates up and down. Yaw-rate information is given by the lower needle, which translates left and right, and roll-rate information is given by the upper needle, which also translates left and right. Full-scale deflections of these needles indicate rates of 6 deg/sec. Pitch attitude is presented by a 360° dial-type instrument located to the right of the center in such a position that at the attitude desired for retro-rocket firing (-43°), the needle will be alined with the zero position for the pitch-rate needle. Yaw attitude is presented by a 360° dial instrument. To the left of the roll-attitude instrument is the acceleration meter, which indicates from -2g to 25g.

<u>Display B</u>.- Figure 4 shows a photograph of display B. This display is identical to display A except for the arrangement of the yaw-rate and roll-rate indicator needles. In this arrangement both of the needles which translate left and right move together to indicate yaw rate. Roll

rate is indicated by a needle which rotates about a pivot point located in the center of the rate display. The pivot point was painted a color that contrasted with the color of the yaw- and pitch-rate needles and served as a zero reference point for these needles.

Display C.- The third type of display utilized in the tests, display C, is shown in figure 5. Attitude information is integrated into what is referred to as a "3-axis eight-ball." The simulated action of the eight-ball is such that it stays alined with a set of axes fixed with respect to the horizon and the local vertical. Angular motion of the capsule results in corresponding angular motions of the eight-ball relative to the instrument case. The resulting angular displacement of the eight-ball gives the pilot an indication of the yaw, pitch, and roll attitude of the capsule. Pitch-rate and yaw-rate needles translating up and down and left and right, respectively, are superposed over the eight-ball with the zero position coinciding with the center of the instrument. Full-scale deflection of these needles usually indicated rates of 15 deg/sec. Roll rate is given by a bar-type indicator immediately below the eight-ball which moves right and left to indicate right and left roll rates. Full-scale deflection usually corresponded to 1 radian/sec.

Display D.- Display D represented a modification of display A to show attitude and rate information summed and presented on what was formerly the rate instrument to provide rate-quickened attitude information. The attitude instruments were not used. This system and results of its use are presented more fully in a following section.

Controllers

The controller specified for the Mercury manual control system is a three-axis mechanically linked type that is designed to be operated by angular motions of the pilot's right hand about axes passing through the wrist for pitch, parallel to and slightly below the forearm for roll, and through the longitudinal axis of the grip for yaw. This controller was not available for most of the test program. Because of the desire to compare operation of a three-axis controller with somewhat more conventional control systems utilizing two axes and a rudder (yaw) pedal, a total of four controllers were used during the simulator tests. These include 2 two-axis controllers and 2 three-axis controllers. They may be described as follows:

Controller A.- Controller A, shown in figure 6, was used to simulate a mechanically linked type of controller operated by the pilot rotating a hand-gripped control stick. Pitch control was obtained by rotations of the control grip, as noted on the figure, about a pivot axis passing through the pilot's wrist. Roll control was obtained by lateral motions of the stick about an axis 2 to 3 inches below and parallel to the forearm. Yaw control was provided by a conventional rudder-pedal arrangement. The controller, which was spring centered about all axes, had full throw forces of about 6 pounds in pitch and 2 pounds in roll. The controller had approximately $\pm 30^\circ$ of travel in pitch-control motion and $\pm 20^\circ$ in roll-control motion. The rudder (yaw) pedal travel was approximately ± 3 inches.

Controller B.- Controller B is similar to the one utilized in the command-controller studies described in reference 4. It has been used in previous simulator studies of piloted reentries described in references 5 and 6 and it was used in the present study to simulate a fly-by-wire control system. This controller, which can be seen in figure 7, consisted of a small shaft with a knob on top. The knob was 4 inches above the pivot point and 2 inches above the box that housed the pivot point and potentiometer pickups. The stick, which was spring centered, was free to move $\pm 20^\circ$ for both pitch and roll control. Maximum force was $2\frac{1}{2}$ pounds. The yaw-control system (rudder pedals) used in conjunction with this controller was the same as that used with controller A.

Controller C.- Controller C was constructed for the present tests and provided for control about all three axes. Pitch control was obtained by rotary motions of the pilot's hand about a pivot point at his wrist. Roll control was obtained by lateral motion about a pivot axis slightly below and parallel to the pilot's forearm, and yaw control by pivoting the grip about an axis through its length. The controller was restrained about all three axes by spring force, and spring detents were used for positive centering. The control throws were approximately $\pm 25^\circ$ for pitch, $\pm 22^\circ$ for yaw, and $\pm 15^\circ$ for roll. Control-force characteristics were roughly equal to those of controller D as given in the description of that controller. The controller, as shown in figure 8, utilized a gimbal system such that the inner gimbal was pitch, the intermediate gimbal was yaw, and the outer gimbal was roll.

Controller D.- Controller D also provided for control about all three axes and was the proposed Mercury manual controller at the time of the tests. Control was obtained in a manner similar to that of controller C. This controller had a gimbal system whose order of rotation was yaw, pitch, and roll. The controller is shown in figure 9. It had throws of approximately $\pm 15^\circ$ in pitch, $\pm 15^\circ$ in yaw, and $\pm 15^\circ$ in roll. The force characteristics of controller D were as follows: Breakout forces of 2 pounds in pitch and yaw and $1\frac{1}{2}$ pounds in roll; full-deflection forces of 6 pounds in pitch and yaw and 4 pounds in roll.

Control Torque Functions

Four different variations of control torque with controller deflection were utilized during the tests. All of these had a maximum torque output of 113 ft-lb for pitch and yaw control and 17 ft-lb for roll control. The control-torque functions are referred to as follows:

(1) Proportion control

(2) Proportion control with dead band

(3) On-off control with dead band

(4) Two step on-off control with dead band L974

The variations of torque with decimal fractions of full control deflection for these four control functions are presented in figure 10.

Pilot Tasks

The specific tasks of the pilot during the three phases of control were as follows:

Orbit.- The task of the pilot during the orbit phase was to maintain the pitch, roll, and yaw attitudes of the capsule within either $\pm 5^\circ$ or $\pm 20^\circ$ of a given value. The runs were of 5 minutes' duration and were made to determine the ease or difficulty of remaining within the specified limits.

Retro-rocket firing.- A simulated retro-rocket maneuver normally consisted of having the pilot control the vehicle from an initial attitude of ψ, ϕ, and θ equal to zero to an attitude of ψ and ϕ equal to zero, θ equal to -43°. After stabilizing at this attitude the pilot said he was ready, and 5 seconds later the retro-rockets were fired. After the firing period the pilot returned to the attitude of ψ, ϕ, and θ equal to zero. The main task of the pilot during the retro-rocket maneuver was to maintain the capsule as close as possible to the attitude $\theta = -43^\circ$, $\psi = 0^\circ$, and $\phi = 0^\circ$ during the application of a series of varying torques about all three axes. The torques simulated the misalinement torques that may be present during the firing of the retro-rockets. It is anticipated that there will be three retro-rockets lasting 10 seconds each, with the three fired sequentially at 5-second intervals. Such an operation gives the possibility of a misalinement torque about all three axes that may change magnitude and direction at each 5-second interval during the 20 seconds of retro-rocket firing. The Mercury capsule specifications for the retro-rocket operation allow for a misalinement torque of up to 90 ft-lb. For the present tests the misalinement torques for a single rocket were 45 ft-lb in pitch and yaw and either 6 ft-lb or 3 ft-lb in roll. Thus, depending upon the direction of the individual rocket misalinements, it is possible that during the period of overlap of firing the misalinement torques may either add to one another or cancel one another. The following table lists the amount of misalinement torque used about each axis for each rocket fired:

Rocket	$M_{X,r}$, ft-lb	$M_{Y,r}$, ft-lb	$M_{Z,r}$, ft-lb
1	±6	±45	±45
2	±3	±45	±45
3	±6	±45	±45

A typical time history of misalinement torques is presented in figure 11 together with an explanatory diagram showing the method of obtaining $M_{Y,r}$ and $M_{Z,r}$. The method for obtaining $M_{X,r}$ was similar. The misalinement-torque values were picked to simulate a situation which was always at least as severe as that specified for the Mercury capsule.

Reentry.- The task of the pilot during the reentry phase was primarily one of stabilization (i.e., to damp any oscillatory tendencies and prevent the motion from reaching large amplitudes). In the initial part of the reentry this task amounted to establishing the yaw and roll attitudes close to zero and the pitch attitude either at zero or at approximately the flight-path angle. As the dynamic pressure built up as a result of increased atmospheric density, the static stability of the capsule tended to establish its correct pitch and yaw attitude and the pilot's task became one of interpreting the rate display so that he could remove energy from any oscillations that developed. There was no static stability in roll, and in most of the runs the pilot tried to maintain the roll attitude at about the same value throughout the run.

Some runs were also made in which the pilot deliberately established a constant roll rate during the initial part of the reentry. This was done in order to average out any out-of-trim lift forces so that the capsule trajectory would still follow a ballistic path. In these runs the pilot, in addition to establishing and maintaining the roll rate, still had the task of damping pitch and yaw motions.

During both types of reentry runs (with and without steady roll) the pilot sometimes purposely excited pitch and yaw oscillations and then attempted to regain control in order to study better the problem of control.

USE OF A RATE-COMMAND SYSTEM FOR CONTROL DURING RETRO-ROCKET FIRING

In the latter stages of the program a rate-command system was added to the simulation. Angular velocities p, q, and r were compared with controller deflections δ_1, δ_2, and δ_3 and the resulting error signals were scaled to command torques to oppose external disturbances. The torque profile utilized was an on-off type with a dead band set at velocities of 1, 1.5, and 2 deg/sec. A hysteresis simulation was used at times with the rate-command system. (See appendix.) The following diagram illustrates the circuits of the rate-command system and type of torque profile commanded.

L
9
7
4

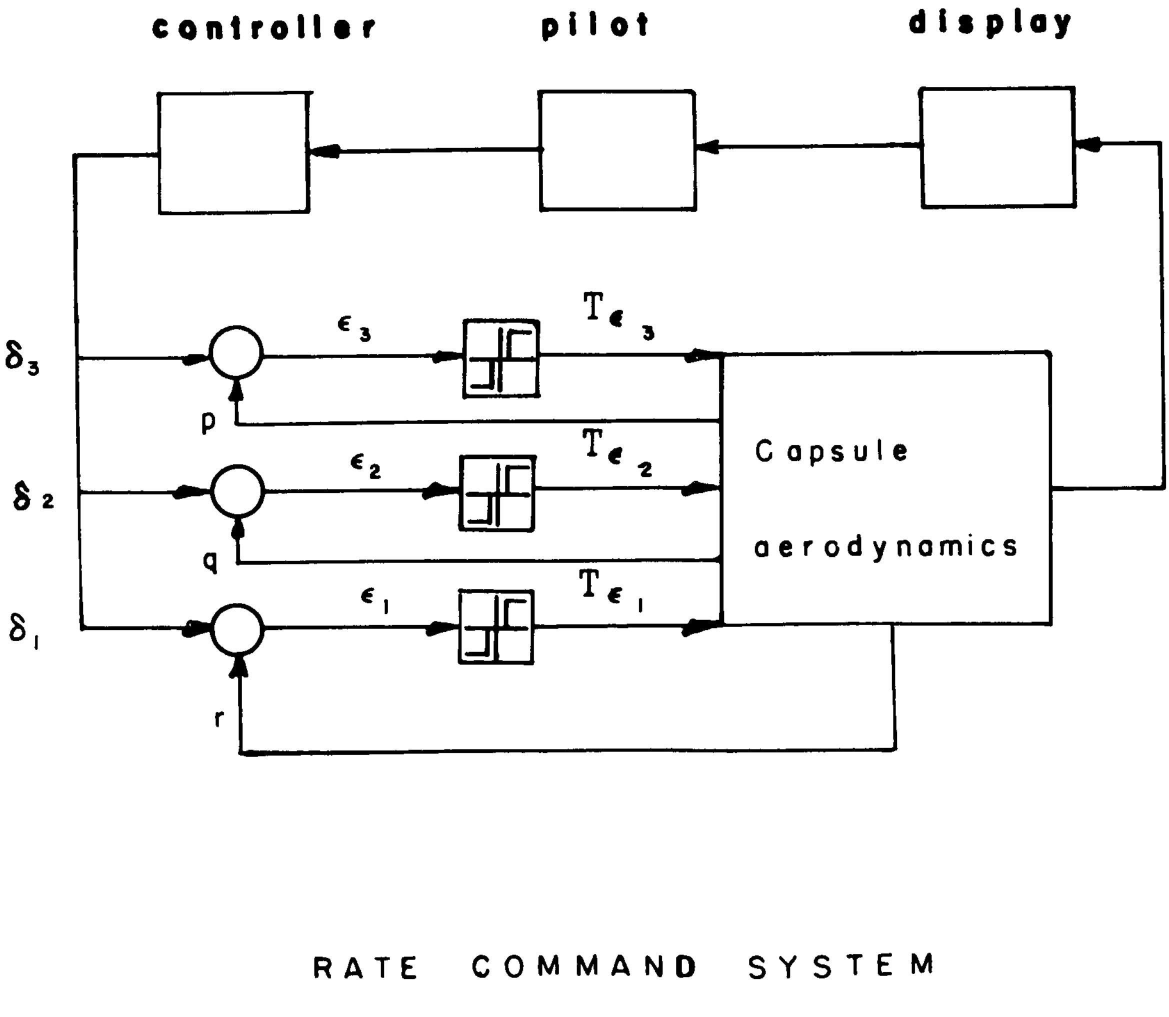

RATE COMMAND SYSTEM

RESULTS AND DISCUSSION

Control During Orbit

General.- After some indoctrination and practice, control of the capsule attitude during orbit was not a particularly difficult problem with any combination of display, controller, and control-torque function. The on-off type of control-torque function provided the least desirable control because of the difficulty in applying the exact amount of torque needed with the resulting tendency to excite more motion than desired. The 3-axis-eight-ball display was preferred over the other displays because it required a much simpler scan pattern.

Fuel expenditure.- Perhaps the best way of evaluating the control-torque functions is by comparing the amounts of fuel expended in 5-minute periods during which the pilot attempts to keep the attitude of the capsule within $\pm 5^\circ$ or $\pm 20^\circ$ limits of a specified orientation. Figure 12 presents a summary of the data obtained on the fuel expended while controlling with various control-torque functions. The data are not sufficient to allow quantitative comparisons; however, the indications are that the two-stage on-off control provides the lowest fuel consumption. Figure 13 shows the fuel consumption for a number of runs in which various combinations of display, controller, and control-torque function were used. The data are distinguished only by the attitude limits maintained and control-torque functions. For the limit of 5° in attitude it appears that approximately 0.45 pound of fuel will be expended during the run, or a rate of 5.4 lb/hr. Increasing the limit to 20° decreased the fuel expenditure to approximately 3.6 lb/hr.

Control During Retro-Rocket Firing

General.- Control during the firing of the retro-rockets was found to be a very difficult task with any combination of instrument display, controller, and control-torque function. It was found that a considerable amount of time was required to become familiar with the display and controller and the requirements for maintaining control. Even when the pilot became relatively adept at controlling this maneuver there were occasions when, because of a mistake in applying control torque or in interpreting the display, control over the attitude was lost. The tests emphasized the need for obtaining a display that presents the important information to the pilot in a manner that is easily and quickly interpreted and in addition a controller which can be readily deflected for control about any axis without inadvertent control about the other axes.

Magnitude of retro-rocket torques which could be controlled.- In order to determine the amount of retro-rocket out-of-trim torques that could be controlled with the control-torque capability of the simulated system, runs were made with successive increases in the magnitude of the imposed torques. One display and controller combination was used: The three-axis-eight-ball with the two-axis mechanically linked controller. For these runs a single retro-rocket (or salvo) was fired for a period of 10 seconds. The maximum that was found to be controllable was a combination of 100 ft-lb in pitch and yaw and 12 ft-lb in roll, which amounts to about 88.5 percent of control capability. Plots of these results appear as figures 14 and 15. Although too few runs were made to be sure, one would expect a rapid increase in the magnitude of the peak excursion as the disturbance torque approaches the control torque available. The data presented in these figures show little change in the magnitude of the peak excursions for values of the ratio of retro-rocket disturbance torque to maximum control torque from 0.50 up to about 0.75. It would again be expected that magnitudes of peak excursions of about 10° would exist about all axes even if the out-of-trim torques were only half, or possibly less, of the available control torque.

Comparison of control-torque functions.- The proportional (with or without dead band) control-torque functions were found to be preferable for controlling a normal retro-rocket run. The reason for this preference is that fewer deliberate control motions were made than with the on-off function. With the on-off function the amount of torque obtained was almost never the exact amount needed at any moment and the pilot had to move the controller in and out of the on-off deflection point in order to balance the disturbance adequately and maintain the proper attitude. Time histories of two runs showing controller displacement when the pilot is using the proportion control with dead band and the on-off control are shown in figure 16.

Comparison of displays.- The difficulty of controlling the retro-rocket misalinement torques has been previously pointed out. All the instrument displays required that the pilot practice a considerable number of retro-rocket runs before satisfactory control could be accomplished. The pilot who made most of the test runs felt that display C, which includes a three-axis eight-ball for attitude information, was the easiest to learn and to interpret. This instrument presented a picture of the capsule attitude at all times and, therefore, made scanning of the panel almost unnecessary. Its interpretation is essentially the same as that of similar instruments (usually only two axis) used in present aircraft. The display of all attitude and rate information except roll rate at one point cannot be overemphasized as a reason for preference of this display in performance of this difficult maneuver.

All the displays were found to be lacking in attitude sensitivity. Positioning in attitude, which is important for the retro-rocket maneuver, could be done with an accuracy of only about $\pm 1\frac{1}{2}^{\circ}$ because of this poor display sensitivity and a small amount of parallax. Since the tolerance desired for attitude control during retro-rocket firing was $\pm 3^{\circ}$, the reading error of $\pm 1\frac{1}{2}^{\circ}$ was significant. Marking the pitch attitude desired for retro-rocket firing was beneficial in providing the pilot with a more easily seen point of reference during the actual firing. The lack of display sensitivity to attitude was especially objectionable during the retro-rocket firing when display A was used, since the pilot's necessarily rapid scan rate did not allow him time to attempt any close interpretation of the attitude display.

Comparison of side-arm controllers.- The pilot found controller C to be a desirable controller for the retro-rocket maneuver in spite of several undesirable (but correctable) features such as excessive flexibility, weak stops, large maximum deflections, and strong spring forces. He also felt that its feeling of flimsiness was a strong psychological deterrent to best task performance. Although controller D was more soundly constructed than controller C, but otherwise similar to it, it did not operate well enough when the tests were run (because of one bad component) to justify any comparison. After making a number of runs with each of the controllers the pilot felt that a well-designed three-axis controller would be at least as satisfactory as a well-designed two-axis controller with rudder pedals for yaw, and perhaps more so. Because so few data were available, it is felt that further testing should be done to corroborate this opinion.

All of the controllers used were found to require undesirably large deflections for maximum control torques. When the retro-rocket out-of-trim torque was a large percentage of the available control torque the pilot often had full, or close to full, control deflection about all three control axes. If the pitch-control deflections were large, a condition of binding of the pilot's wrist sometimes hampered his roll-control motions (and yaw control in the case of the three-axis controller). This problem would probably be more acute under the accelerations imposed by the retro-rocket. Limiting the controller angular deflections to 10° or 15° should alleviate this trouble.

Accuracy of control.- The accuracy with which the retro-rocket maneuver could be controlled was somewhat inconsistent, probably because of the random selection of direction for the individual rocket misalinement torques and the apparently critical nature of variations in the pilot's response time. A fairly good indication of the accuracy of control was obtained by determining the maximum peak-to-peak excursion of each of the three attitude parameters. This information is presented in summary form in figures 17 and 18. The data points which are flagged indicate runs in which the attitude exceeded the recorder limits ($\psi = 25^\circ$, $\theta = 100^\circ$, $\phi = 50^\circ$) in at least one direction. The average maximum excursions are indicated by the short horizontal lines. It should be kept in mind when making comparisons among the figures that there was considerable improvement due to learning over the period of the tests. The runs with display C shown in figure 18(b) were among the earliest, and despite wide differences from run to run the accuracy of control with display C was better than that with any of the other combinations unless the rate-command system was used. Note that the average excursions in pitch and yaw never exceeded 20° for these runs. Although too few runs were made to allow specific conclusions, it appears from figure 17(b) that the modification made to display A was of help to the pilot in controlling the vehicle. It is noticed when display B is compared with display A that the average excursions with the former were lower except in pitch in one case. Furthermore, and probably more important, the pilot's performance was usually more consistent with display B. Accuracy of control in the important modes of pitch and yaw with display B could not, however, compare with that of display C. In figure 17 this fact is illustrated by the clear difference in performance when these two displays are compared. There were few retro-rocket runs with the standard test magnitude of out-of-trim torques in which the pilot was able to control within the design specification attitude limits of $\pm 3^\circ$. Figure 19 indicates that use of peak attitude rather than peak-to-peak excursions is also an acceptable way of judging attitude error and as such does not give significantly different results from the peak-to-peak excursions. This figure is based on the same data as figure 17(b). Because the attitude during the retro-rocket firing must be held within fairly close limits in order to obtain desired initial reentry angles and to arrive at the desired landing area, it is apparent that the manual retro-rocket control problem needs added attention in order to arrive at a satisfactory solution.

Control with quickened display.- As an incidental test in the investigation of control during retro-rocket firing, several runs were made in which both attitude and rate information were combined and presented by a single needle indicator for each axis, in somewhat the manner of the tests described in reference 7. In these runs the rate instrument of display A was used to show both rates and attitude. These were summed about each axis and displayed in the following relationship: Full-scale needle deflection = 6 deg/sec of rate or $22\frac{1}{2}^\circ$ of attitude $\left(\text{alternatively, } 11\frac{1}{4}^\circ\right)$ or equivalent combinations of lower values. Runs made with this modification showed that although the impression given to the pilot is that of having performed more poorly than when using more conventional displays, he actually did as well as or better than in his other runs. With the higher attitude sensitivity $\left(11\frac{1}{4}^\circ = \text{full-scale attitude signal}\right)$ both of these effects were more pronounced. Results of these tests are presented in figure 20.

Control with a simple rate-command system.- Another incidental series of runs during the investigation was made by using the deflections of a three-axis controller to command rates of capsule angular motion. Though not compatible with a mechanically linked control system, such a system might be a solution to the problem of control during a retro-rocket firing. Rate-command loops were used for motion about all three axes in the manner outlined in the description, and several retro-rocket runs were made. Such a system simplified the pilot's job to one of monitoring the run and adding control input to take care of the small rates associated with the dead band in the control torque function. The test whose time history appears in figure 21 was made with a control gain of 20 deg/sec for maximum control deflection, nominal dead band of 1 deg/sec, and hysteresis of 50 percent (see appendix). Although a number of runs were made with different values of these parameters, the results were not significantly different. It is apparent from the figure that control during retro-rocket firing was radically improved, and analysis of several runs showed that the pilot consistently stayed within $\pm 3^{\circ}$ of the desired attitude.

Control During Reentry

General.- Previous studies of pilot-controlled reentry (refs. 5 and 6) have indicated that under conditions of zero damping the pilot control problem was critical. The reasons for this critical condition have been given as inadvertent cross-control application, a destabilizing effect due to decreasing dynamic pressure (after the point of peak deceleration), and inertia coupling. In the present study the problem of pilot control during the reentry was not found to be critical. In fact, in many runs the pilot purposely excited pitch and yaw oscillations so that he could better evaluate the use of various controllers and instrument displays, and he was able to regain control in most cases quite readily. The difference in the results of the present tests and those of previous studies of piloted reentries is probably due to several factors. One of these factors is that the present tests utilized instrument displays that included angular rate information and this simplified the pilot's task of damping oscillations. Another factor is that the simulation of reference 5 used approximations for α and β which did not allow for effects due to rolling and yawing motions, and used small-angle approximations in computing the Euler angles. These small-angle approximations and the α approximation were introduced into the present equations in order to determine what, if any, effect they had on the difficulty of control. It was found that this change did cause the reentries to become much more difficult to control.

Comparison of displays, controllers, and control torque functions.- The pilot was able to maintain control during the reentry phase with any combination of display, controller, and control torque function that was tested. There were no important differences in control attributable to differences in instrument display, although the pilot preferred display B to display A on the basis of ease of interpretation of the rate indicators. There were also no important differences attributed to controllers, although the lack of positive centering in controllers A and B was annoying because of the possibility of inadvertent cross control. There was a definite preference for the proportion control torque function (either with or without dead band) over the on-off type since the proportion function allowed the pilot some control over the magnitude of control torque. There was also less tendency to excite undesirable motion with the proportion torque function.

L
9
7
4

<u>Effect of excluding angular rates from instrument display</u>.- The importance of the angular-rate information to the pilot during the reentry phase may be seen by comparing the time histories of runs made with and without rate information. Such runs are presented in figures 22 and 23. While the pilot was able to maintain control in both cases, the display of rate information allowed him to damp oscillations which it was impossible for him to see otherwise. In the figures this may appear to have been unimportant since the oscillations were of small amplitude. However, during some runs in which the pilot purposely excited oscillations, the time to regain control was extended when no rate information was displayed, and the damping of the oscillations required more diligence on the part of the pilot in order to time properly his control inputs.

<u>Effect of steady roll rates upon yaw and pitch control</u>.- In a number of runs, as the deceleration first began to increase the pilot initiated a steady rolling motion. In most cases the rate of roll was held at about 1/2 radian/sec, although in some runs a lower rate was used. The purpose of such a maneuver is to average out any lift forces generated by the capsule so that it will follow a ballistic trajectory through the atmosphere to a predicted range. The rolling velocities used were probably greater than those required to average out the lift forces and therefore served to exaggerate any problems involved in such a maneuver.

When the trim angles of attack and sideslip were zero the pilot experienced no difficulty of control during the initiation of the roll or the steady rolling portion. His interpretation of the yaw and pitch rate information (necessary for the pilot if he is to supply damping) was no different from that during a normal nonrolling reentry. Even after moderate-amplitude oscillations had been purposely excited the pilot did not experience any particular difficulties in regaining control.

When the trim angles of attack and sideslip were set to values of $\pm 5^\circ$ or $\pm 10^\circ$ the information from the instrument display was more complicated and the problem of control slightly more difficult. In these cases the capsule tended to roll about the wind axis rather than body axis and components of the resulting angular velocity were present about both the pitch and yaw axes. Superimposed on these steady rates were the oscillations associated with natural frequencies in pitch and yaw. An example of the motion is shown in the time history presented in figure 24. In spite of this rather complicated motion the pilot was able to control most of the reentry runs that were made with the higher values of trim angle of attack and sideslip. In a few runs where α_T and β_T were 10°, after the peak acceleration was passed the pilot was unsuccessful in keeping the magnitude of the oscillations sufficiently low and he ultimately lost control of the capsule. Even at the lower values of α_T and β_T, if the pilot excited an oscillation of moderately large amplitude after the peak acceleration was passed it was possible that he would lose control. Such a condition might come about unintentionally, but it occurred only as a result of intentional disturbances when α_T and β_T were less than 5°.

CONCLUSIONS

As a result of analog-simulator studies of pilot manual control of a capsule-type vehicle during orbit, retro-rocket firing, and reentry the following conclusions were drawn:

1. The most difficult phase of control is during the firing of the retro-rocket and results from the large disturbances of the misalinement torques.

2. The pilot was seldom able to control the capsule attitude during retro-rocket firing to within the $\pm 3^{\circ}$ design specification limits without making use of a rate-command control system.

3. A simplified rate-command control system enables the pilot to maintain attitude control during the retro-rocket firing to within the $\pm 3^{\circ}$ design specification limit.

4. Control of the capsule during a normal reentry was not a particularly difficult task when rate information was supplied to the pilot.

5. The pilot could maintain satisfactory control during reentry when the capsule was made to roll at steady rates except when trim angle of attack and sideslip became large (of the order of $\pm 10^{\circ}$).

6. A three-axis side-arm controller similar to the one used in the tests, but with some design improvements, could provide a desirable control input system.

7. Display B was generally satisfactory but lacked the integrated display advantage of display C.

8. The proportion control torque function with dead band was generally the most desirable of the control-torque functions tested.

Langley Research Center,
National Aeronautics and Space Administration,
Langley Field, Va., May 17, 1960.

L
9
7
4

APPENDIX

DISCUSSION OF THE ANALOG SIMULATION OF THE VEHICLE DYNAMICS

This appendix, in a chronological order, presents some problems encountered in the analog simulation of the vehicle dynamics. A 1:1 time solution of the equations of motion was obtained to allow a pilot to close the loop between the computer and the cockpit. A schematic diagram of the analog simulation is shown in figure 25. Table I and table II give potentiometer settings, gains, and amount of equipment used in the programing of the simulation. The following block diagram shows the information flow of the computer program.

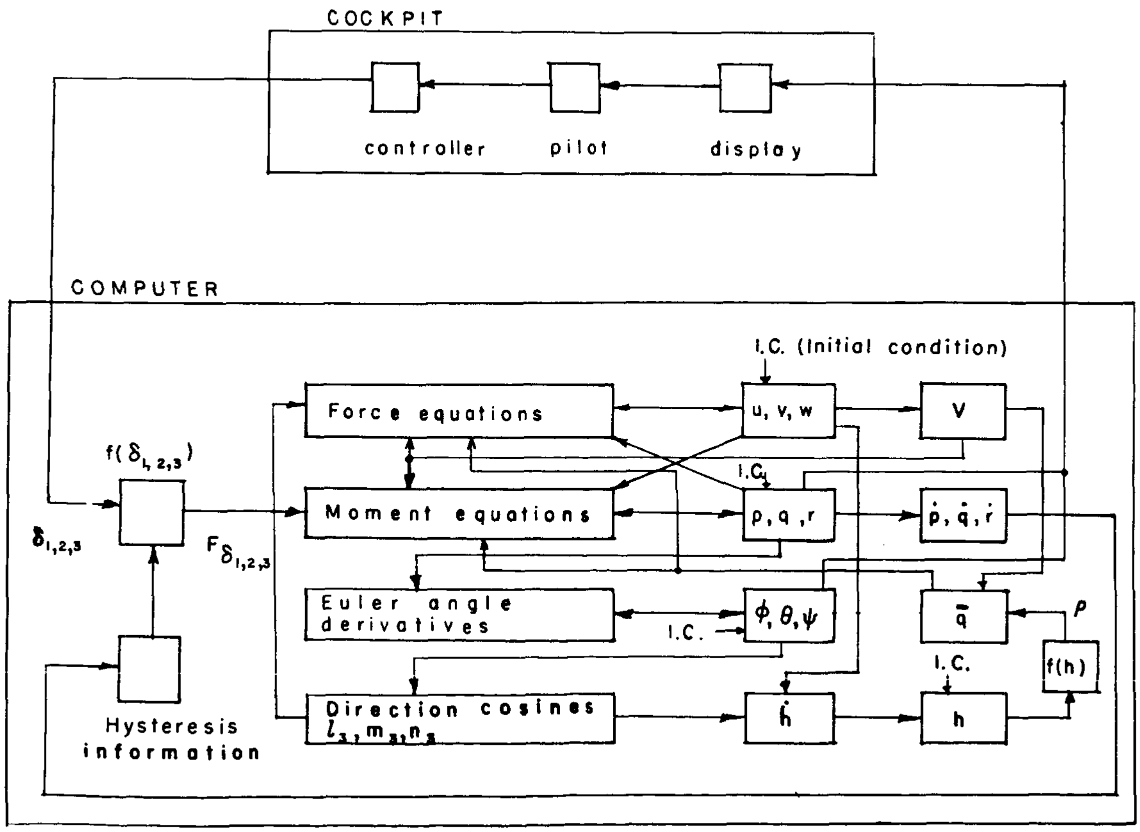

Position resolvers available are mechanically limited to $\pm 180^\circ$ and conditions of the problem required that the roll angle ϕ obtain a magnitude of $4{,}000^\circ$. Continuous resolution of ϕ was required and was accomplished through the use of sine and cosine oscillators. The technique is based on the solution of the differential equation

$$\frac{d^2x}{d\phi^2} + x = 0 \tag{18}$$

The solution with initial condition $x(0) = 0$ and $\frac{dx}{d\phi}(0) = 1$ is $x = \sin\phi$ and $\frac{dx}{d\phi} = \cos\phi$. The electronic analog integrates with respect to time; therefore, one can multiply the integrand by $\frac{d\phi}{dt}$ and the integration with respect to ϕ is accomplished. For example,

$$\int z \frac{d\phi}{dt}\, dt = \int z\, d\phi \tag{19}$$

The resolver equations to be solved are:

$$\frac{d}{dt}(\sin\phi) = \frac{d\phi}{dt}\cos\phi - k(\sin^2\phi + \cos^2\phi - 1)\sin\phi \tag{20}$$

$$\frac{d}{dt}(\cos\phi) = -\frac{d\phi}{dt}\sin\phi - k(\sin^2\phi + \cos^2\phi - 1)\cos\phi \tag{21}$$

The use of equations (18) and (19) to obtain the sine and cosine of ϕ is satisfactory for a small number of cycles, but if many cycles are required the errors caused by integrator drift and servomultiplier positioning must be eliminated. The trigonometric identity

$$\sin^2\phi + \cos^2\phi = 1 \tag{22}$$

will not be an equality because of these errors. To counter them, correction terms $-k(\sin^2\phi + \cos^2\phi - 1)\sin\phi$ and $-k(\sin^2\phi + \cos^2\phi - 1)\cos\phi$ are added, as shown in equations (20) and (21). The analog circuits involved in the solution are shown in the following diagram:

DECL[redacted]IED

L-974

Let $\epsilon = \cos^2\phi + \sin^2\phi - 1$

$$\dot{\phi} = \frac{d\phi}{dt}$$

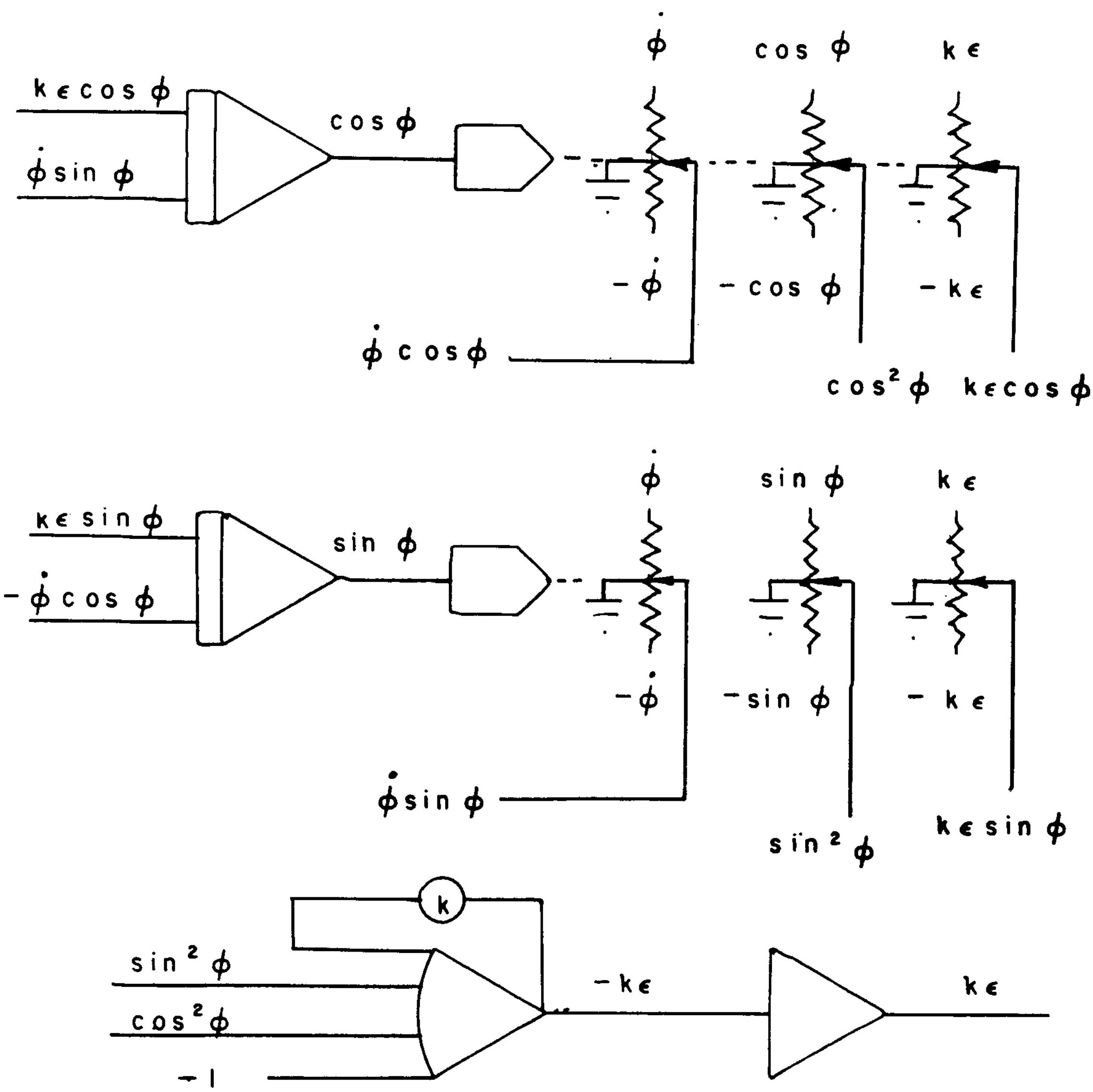

[redacted]

A correct entry is dependent upon the accurate computation of $\dot{h}$, which consists of l_3u, m_3v, and n_3w. A technique utilized to improve the accuracy in the computation of the terms making up $\dot{h}$ was to drive a servomultiplier with the larger voltage and apply the smaller voltage to the multiplying potentiometers of the servomultiplier. When l_3 was zero, the product of l_3u was assured of being zero. For example,

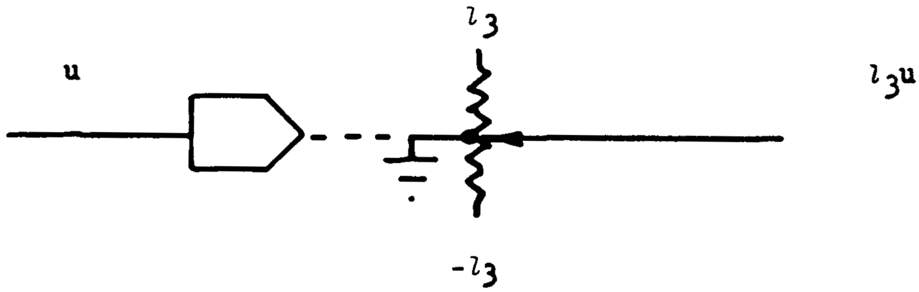

Another problem encountered was the generation of $\bar{q}$. The altitude range as dictated by the problem yielded a density variation of 10^6. Since the computing voltage available is ±100 volts, the voltage representing most of the curve would be negligible for computing purposes. Therefore $\rho^{1/4}$ is generated to compute $\bar{q}$ and the $\rho^{1/4}$ curve represents a change of 10^2, well within computing range. The diagram below shows successive multiplications to compute $\bar{q}$:

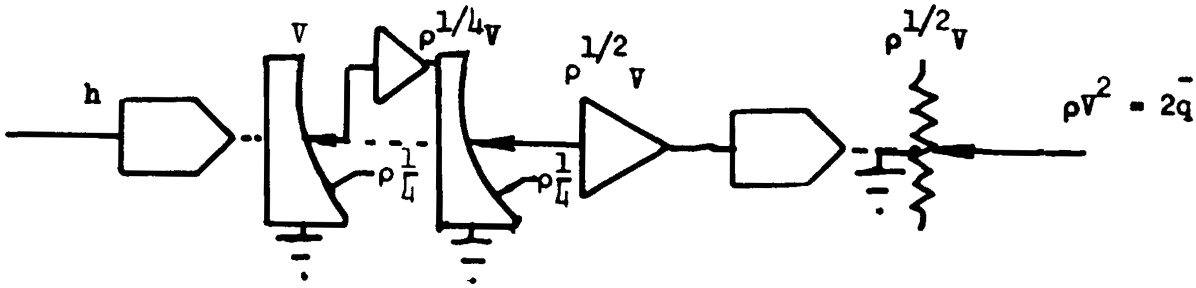

Relay and differentiation circuits were used to simulate hysteresis in the rate-command-system control modes. It was necessary to use $\dot{p}$, $\dot{q}$, and $\dot{r}$ to drive relay circuits in the process of simulating hysteresis. This circuit is as follows:

[redacted]

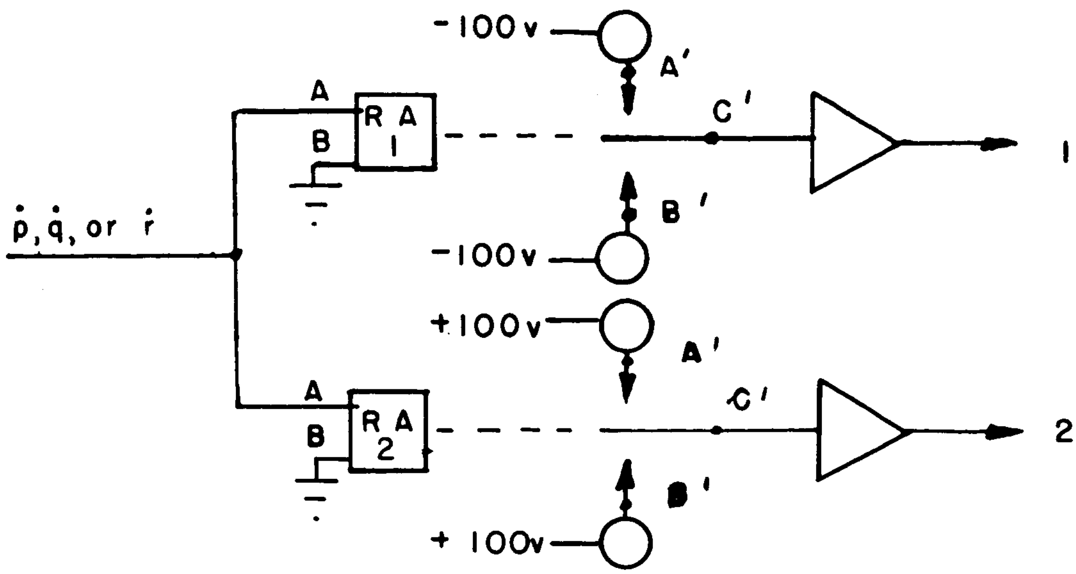

When $\dot{p}$, $\dot{q}$, or $\dot{r}$ is a positive voltage, an A'C' connection is completed and some predetermined voltage will appear at points 1 and 2. Some other predetermined voltage will appear at points 1 and 2 when $\dot{p}$, $\dot{q}$, or $\dot{r}$ is negative because of a B'C' connection at the output of the relay amplifiers. The voltages from points 1 and 2 are used as comparative voltages in the following diagram:

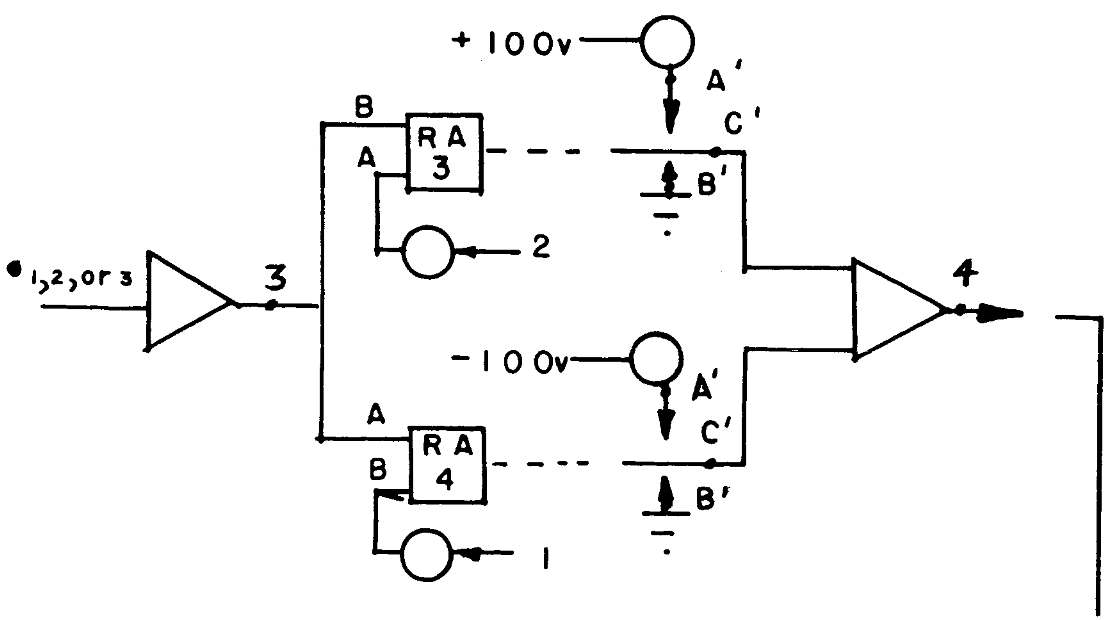

When the error signal ϵ at point 3 is a positive voltage and is larger than the voltage at point 1, an A'C' connection is made at the contact points of relay amplifier 4 and a positive control torque will appear at point 4. If the error signal ϵ at point 3 is a negative voltage and is a larger negative voltage than the voltage at point 2, an A'C' connection is made at the contact points of relay amplifier 3 and a negative torque will appear at point 4. A B'C' connection will be made at the contact points of relay amplifier 3 when an A'C' connection is made at relay amplifier 4. Conversely, when a B'C' connection is made at relay amplifier 4, an A'C' connection will be made at relay amplifier 3. The following torque profile will be generated as a result of the preceding circuits:

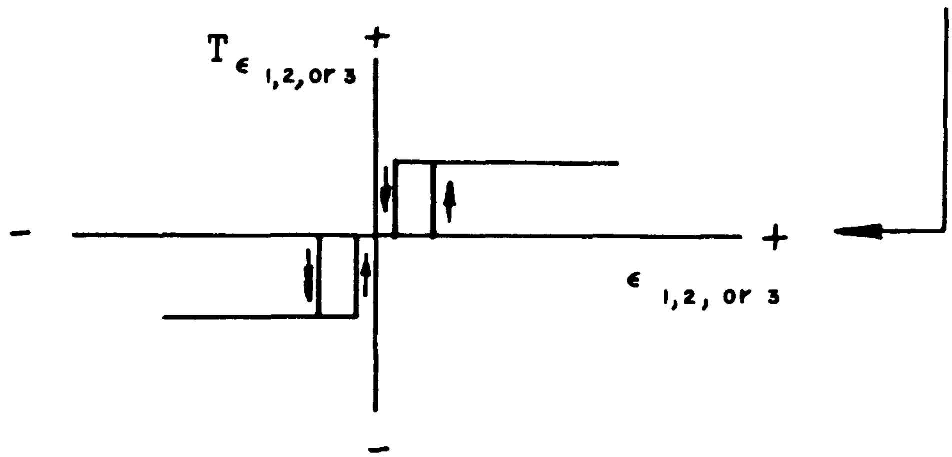

[redacted]

REFERENCES

1. Stillwell, Wendell H., and Drake, Hubert M.: Simulator Studies of Jet Reaction Controls for Use at High Altitude. NACA RM H58G18a, 1958.

2. Etkin, Bernard: Dynamics of Flight. John Wiley & Sons, Inc., c.1959.

3. Assadourian, Arthur, and Cheatham, Donald C.: Longitudinal Range Control During the Atmospheric Phase of a Manned Satellite Reentry. NASA TN D-253, 1960.

4. Sjoberg, S. A., Russell, Walter R., and Alford, William L.: Flight Investigation of a Small Side-Located Control Stick Used With Electronic Control Systems in a Fighter Airplane. NACA RM L56L28a, 1957.

5. Eggleston, John M., Baron, Sheldon, and Cheatham, Donald C.: Fixed-Base Simulation Study of a Pilot's Ability To Control a Winged-Satellite Vehicle During High-Drag Variable-Lift Entries. NASA TN D-228, 1960.

6. Cheatham, Donald C., Young, John W., and Eggleston, John M.: The Variation and Control of Range Traveled in the Atmosphere by a High-Drag Variable-Lift Entry Vehicle. NASA TN D-230, 1960.

7. McKee, John W.: Single-Degree-of-Freedom Simulator Investigation of Effects of Summing Display-Instrument Signals on Man-Machine Control. NASA TN D-148, 1959.

[redacted]

TABLE I.- POTENTIOMETER SETTINGS

Potentiometer	Setting	Gain
1	1.000	1
2	.358	4
3	1.000	1
4	.0763	1
5	1.000	Relay amplifier
6	1.000	Relay amplifier
7	.0763	1
8	0	1
9	0	Relay amplifier
10	0	Relay amplifier
11	0	1
12	1.000	1
13	1.000	1
14	0	10
15	p_o	Initial condition
16	1.000	1
17	L_p	4
18	.380	1
19	.573	10
20	1.000	1
21	.132	1
22	1.000	Relay amplifier
23	1.000	Relay amplifier
24	.132	1
25	0	1
26	0	Relay amplifier
27	0	Relay amplifier
28	0	1
29	1.000	1
30	.250	4

L974

[redacted]

DECL[redacted]IED

TABLE I.- POTENTIOMETER SETTINGS - Continued

Potentiometer	Setting	Gain
31	0	10
32	q_o	Initial condition
33	.891	20
34	1.00	1
35	M_q	4
36	1.00	1
37	.573	4
38	1.000	1
39	.260	1
40	1.000	Relay amplifier
41	1.000	Relay amplifier
42	.260	1
43	0	1
44	0	Relay amplifier
45	0	Relay amplifier
46	0	1
47	.100	10
48	.250	4
49	0	10
50	r_o	Initial condition
51	.931	1
52	.878	10
53	1.00	1
54	N_r	4
55	.573	Servo potentiometer
56	.573	Servo potentiometer
57	.573	Servo potentiometer
58	.573	Servo potentiometer
59	.245	Servo potentiometer
60	.245	Servo potentiometer

[redacted]

L
9
7
4

TABLE I.- POTENTIOMETER SETTINGS - Continued

Potentiometer	Setting	Gain
61	0.063	Servo potentiometer
62	.063	Servo potentiometer
63	$\cos \phi_o$	Initial condition
64	.8726	4
65	.2865	Servo potentiometer
66	.2865	Servo potentiometer
67	.900	Servo input
68	.355	10
69	.2865	1
70	$\sin \phi_o$	Initial condition
71	.8726	4
72	.2865	Servo potentiometer
73	.2865	Servo potentiometer
74	θ_o	Initial condition
75	ψ_o	Initial condition
76	1.000	1
77	.835	4
78	.328	Potentiometer
79	.100	1
80	h_o	Initial condition
81	.760	10
82	.708	1
83	.609	1
84	.888	1
85	.427	4
86	.0095	1
87	.100	Potentiometer
88	.013	1
89	.024	1
90	u_o	Initial condition

TABLE I.- POTENTIOMETER SETTINGS - Continued

Potentiometer	Setting	Gain
91	0.500	1
92	.500	1
93	.025	1
94	.0125	1
95	.0125	1
96	.025	1
97	.833	4
98	.100	Potentiometer
99	.036	1
100	.0095	1
101	.100	Potentiometer
102	.0315	1
103	v_o	Initial condition
104	.300	Servo potentiometer
105	.300	Servo potentiometer
106	.500	1
107	.500	1
108	.050	1
109	.025	1
110	.025	1
111	.050	1
112	.666	10
113	.0095	1
114	.100	1
115	w_o	Initial condition
116	.0315	1
117	.0395	1
118	.600	Servo potentiometer
119	.600	Servo potentiometer
120	.500	1

TABLE I.- POTENTIOMETER SETTINGS - Concluded

Potentiometer	Setting	Gain
121	0.500	1
122	.040	1
123	.020	1
124	.020	1
125	.040	1
126	.090	1
127	.2865	Recorder
128	β_T	1
129	.600	1
130	.600	1
131	α_T	1
132	.2865	Recorder
133	.027	1
134	.0531	1
135	.1042	1
136	.0134	1
137	.0531	1
138	.1042	1
139	.027	1
140	.0531	1
141	.1042	1
142	.557	Recorder
143	.500	Servo input
144	.111	1
145	.100	1
146	ϕ_o	Initial condition
147	ϕ_o	Initial condition
148	.0098	1
149	.0115	1
150	.0228	1

L
9
7
4

TABLE II.- ANALOG EQUIPMENT USED

Components	Number used
Resolvers	1
Servomultipliers	16
Relay amplifiers	21
Integrators	20
Summers and inverters	86
Coefficient potentiometers	150
Recording channels	20

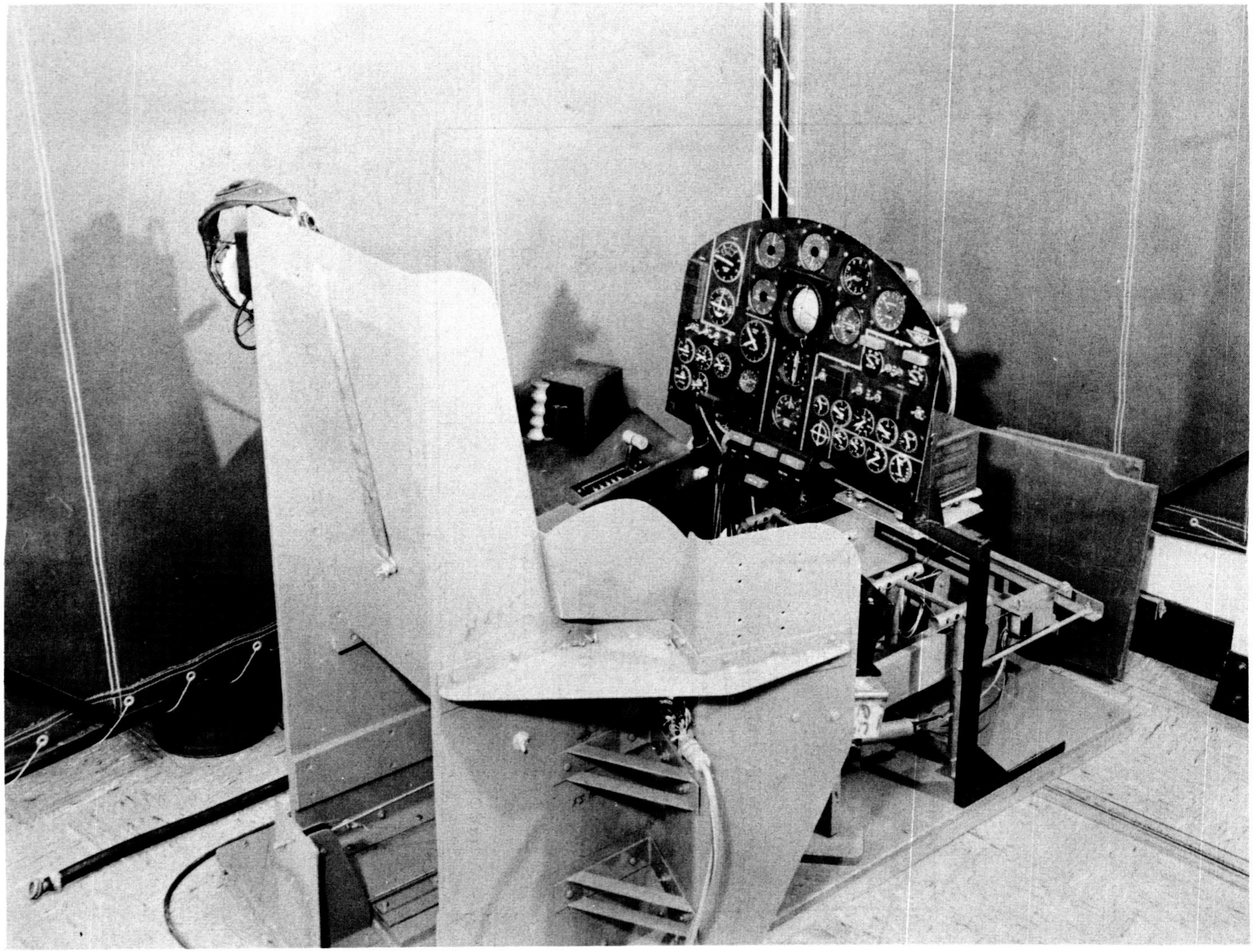

Figure 1.- Simulated cockpit used in tests. L-59-236

L-974

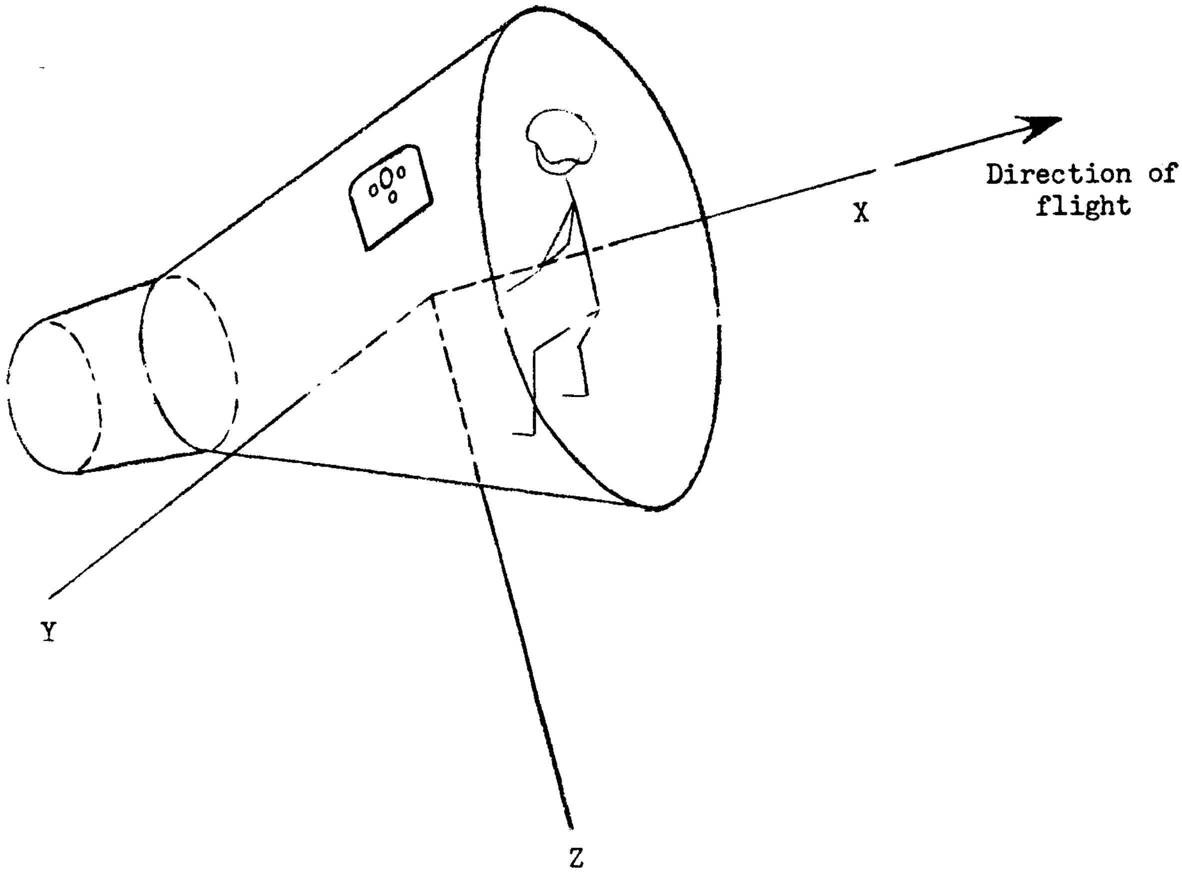

Figure 2.- Position of pilot relative to body axes and direction of flight.

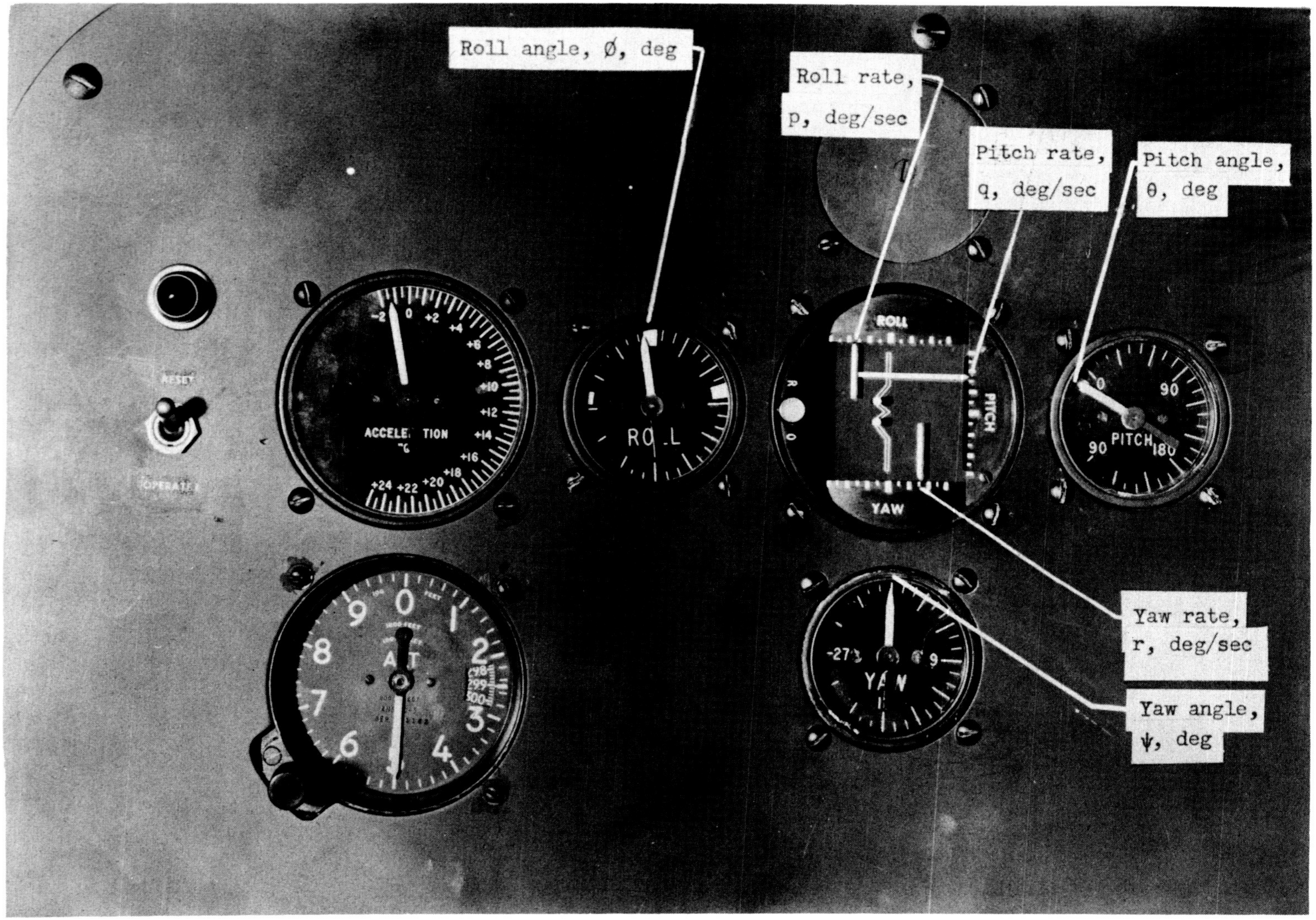

Figure 3.- Display A. L-59-7175.1

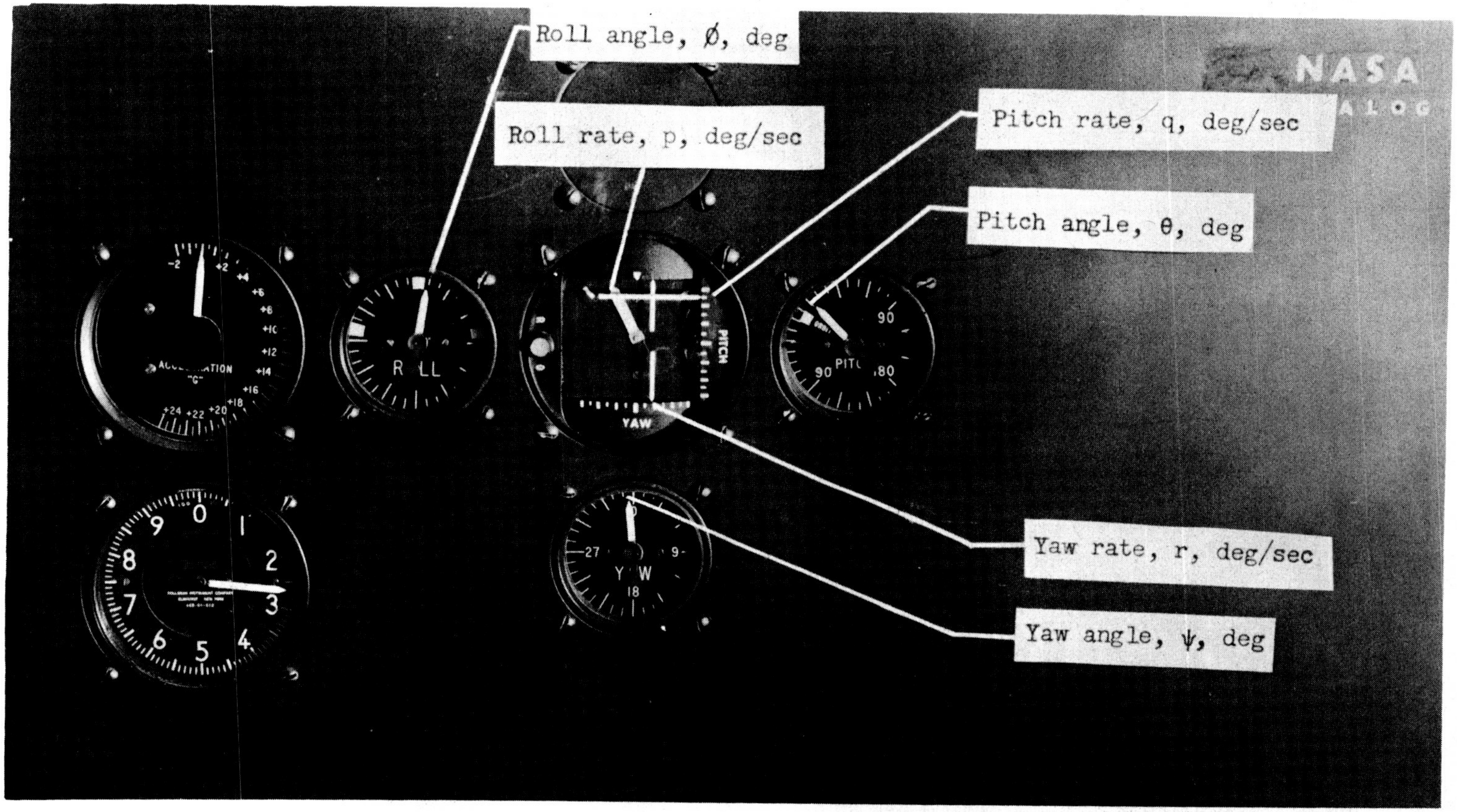

Figure 4.- Display B.   L-59-7126.1

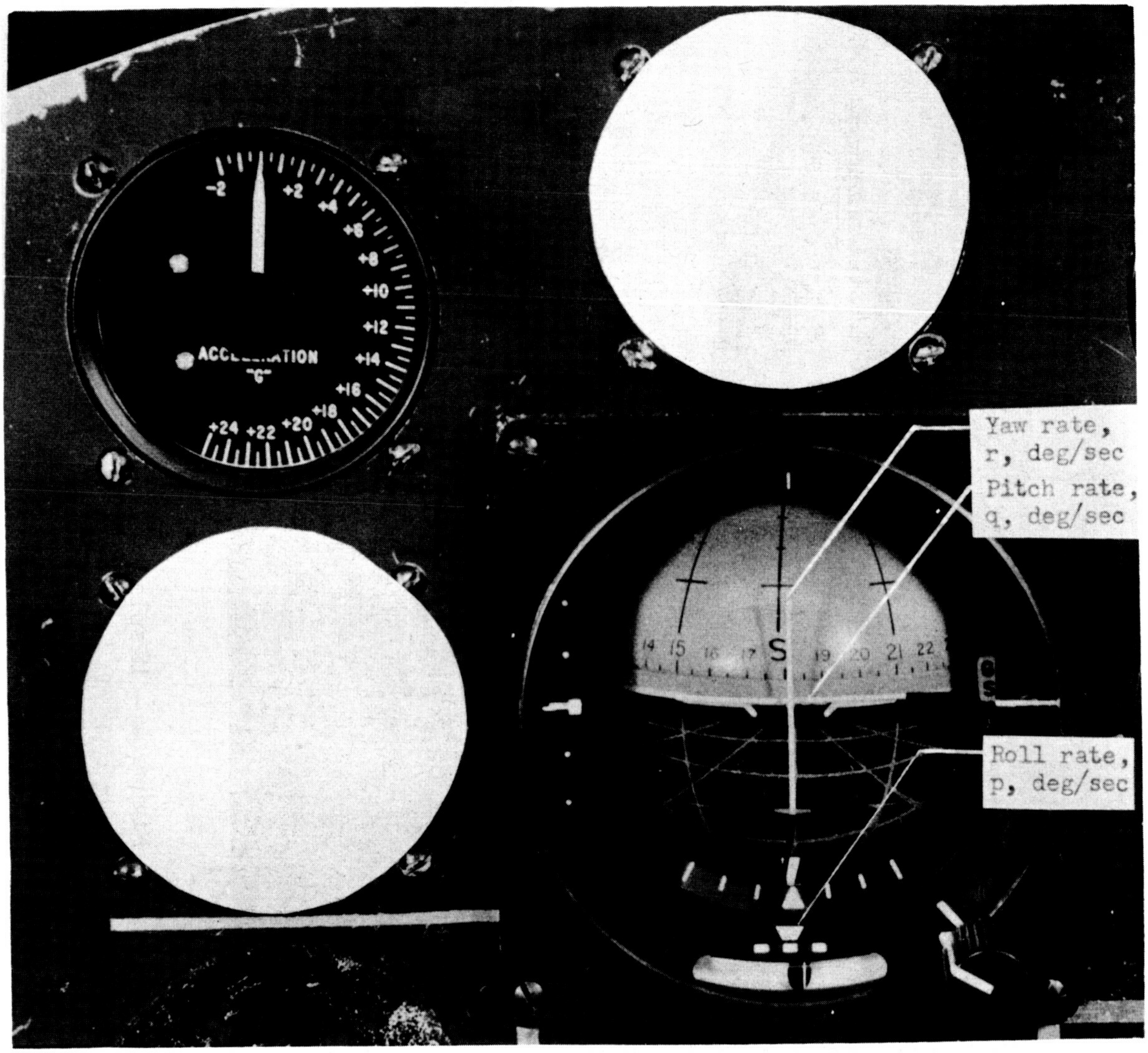

Figure 5.- Display C. L-59-4227.1

L-974

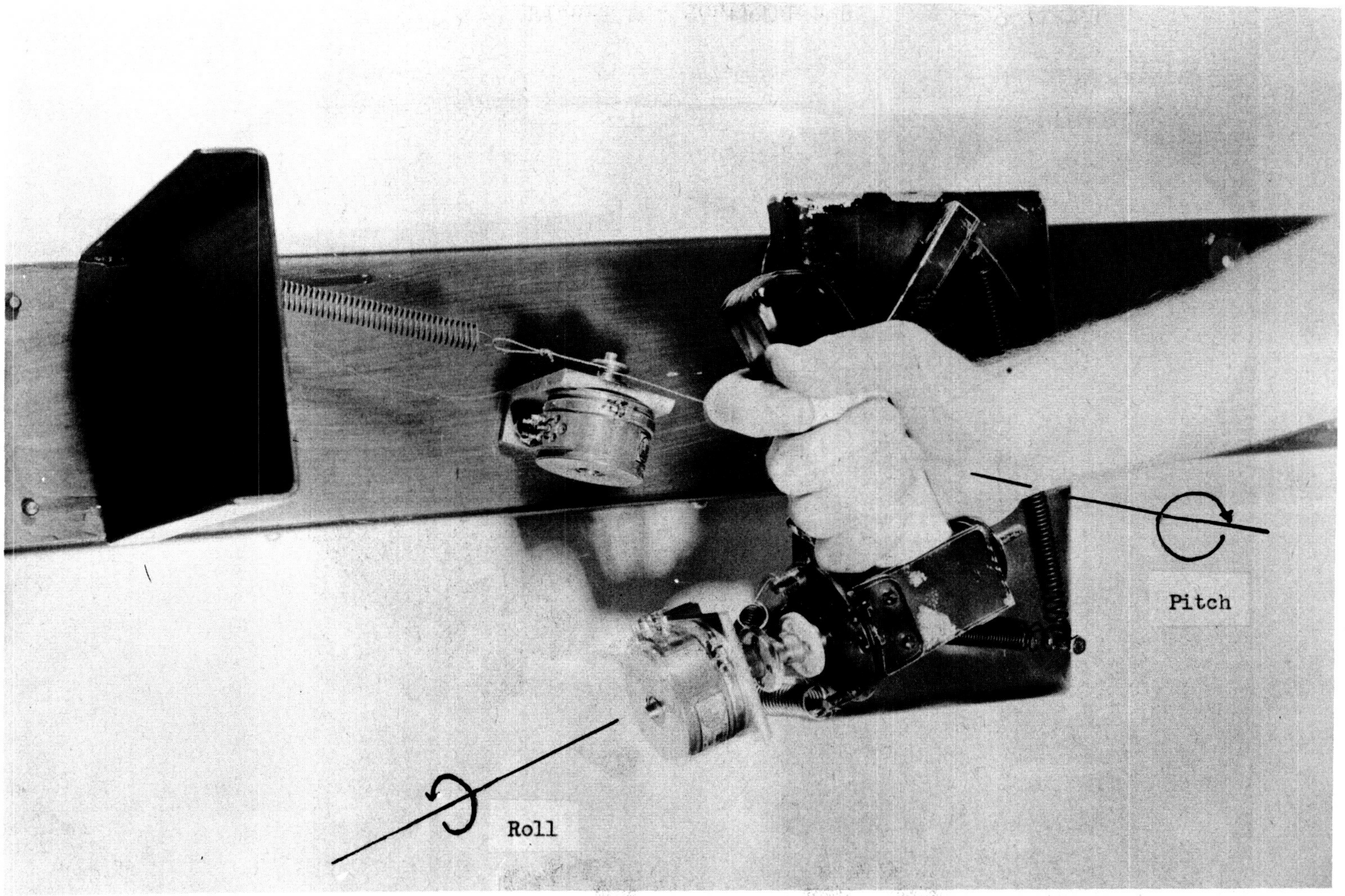

Figure 6.- Controller A. L-59-7174.1

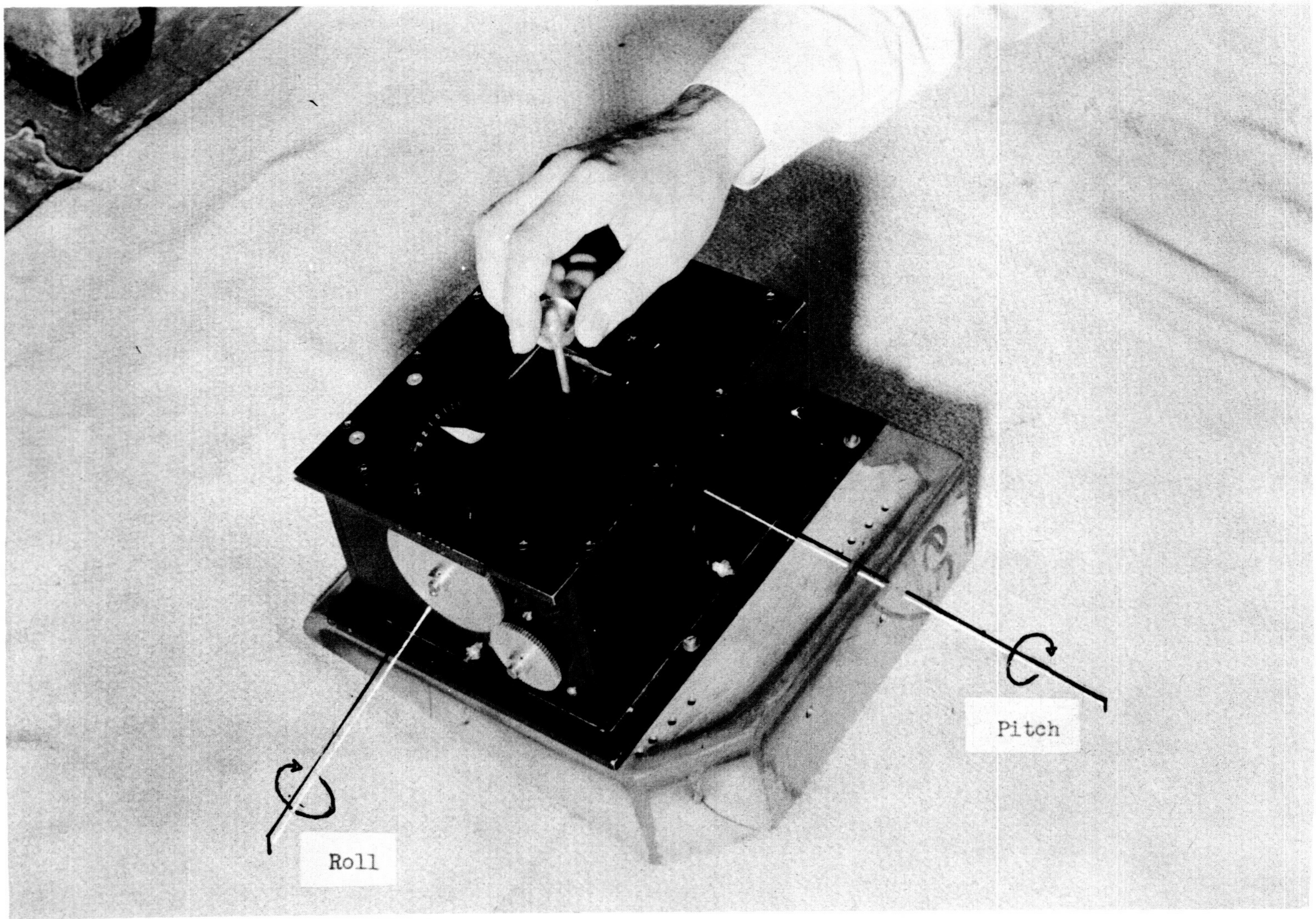

Figure 7.- Controller B. L-59-7125.1

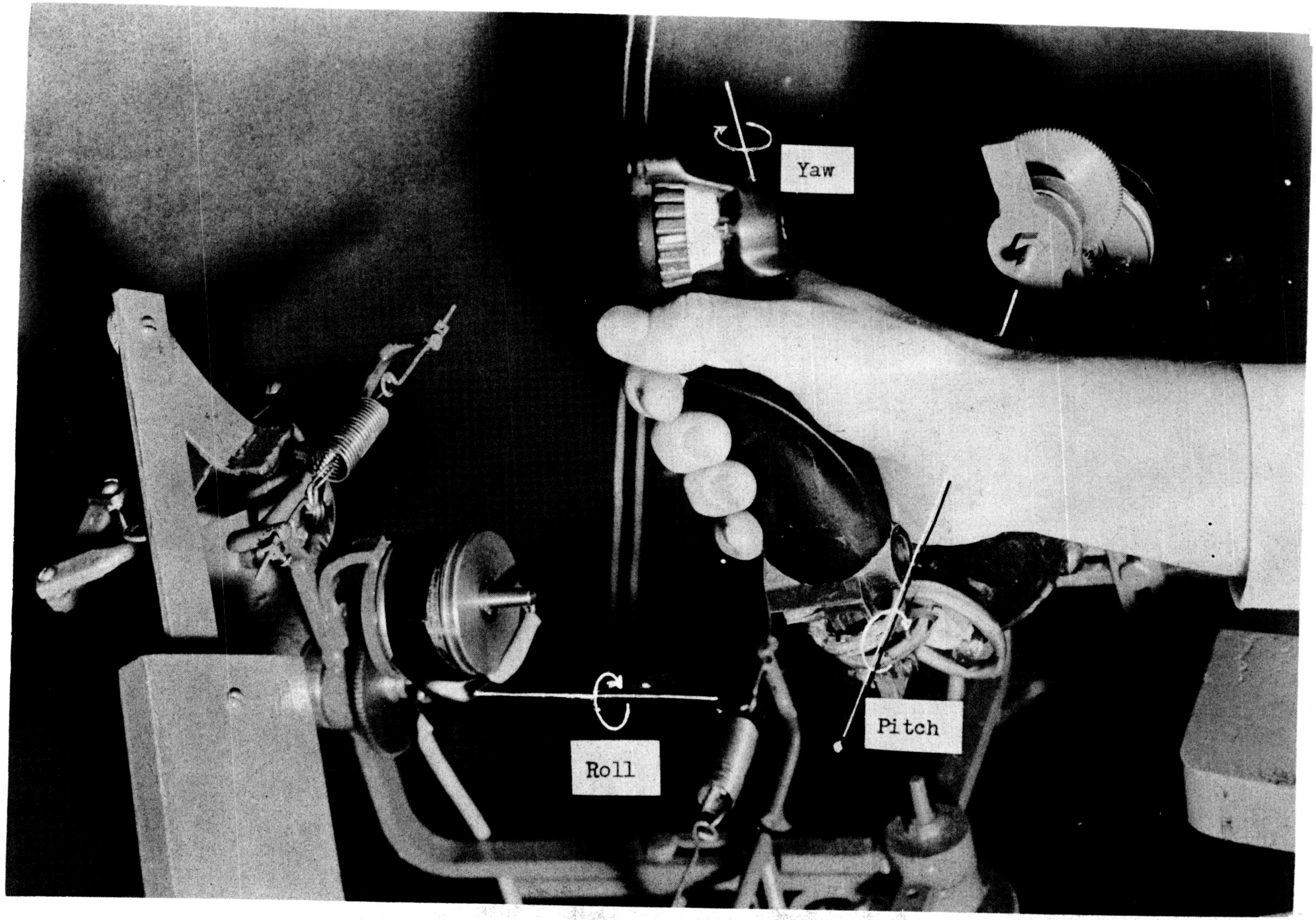

Figure 8.- Controller C. L-59-7123.1

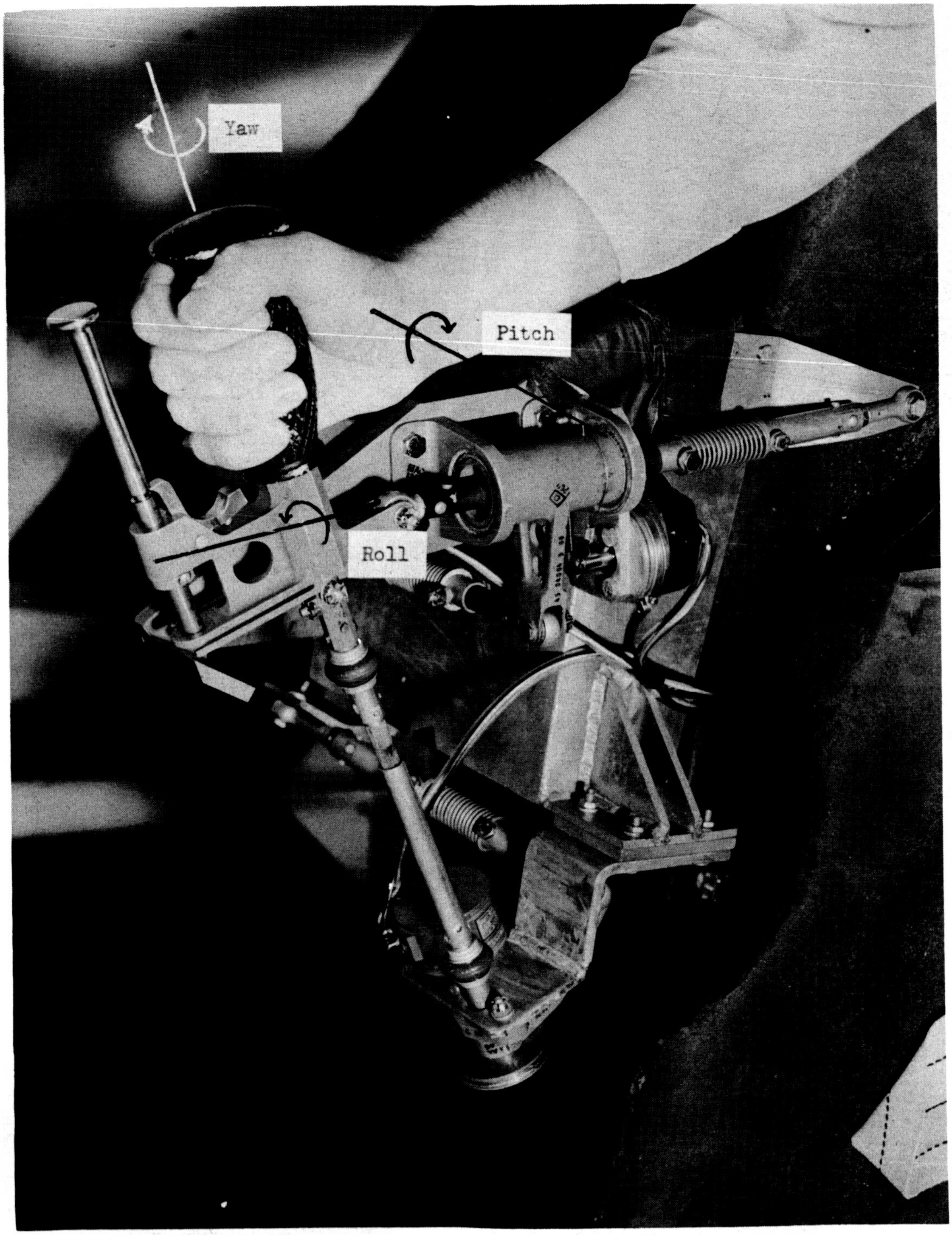

Figure 9.- Controller D. L-59-7121.1

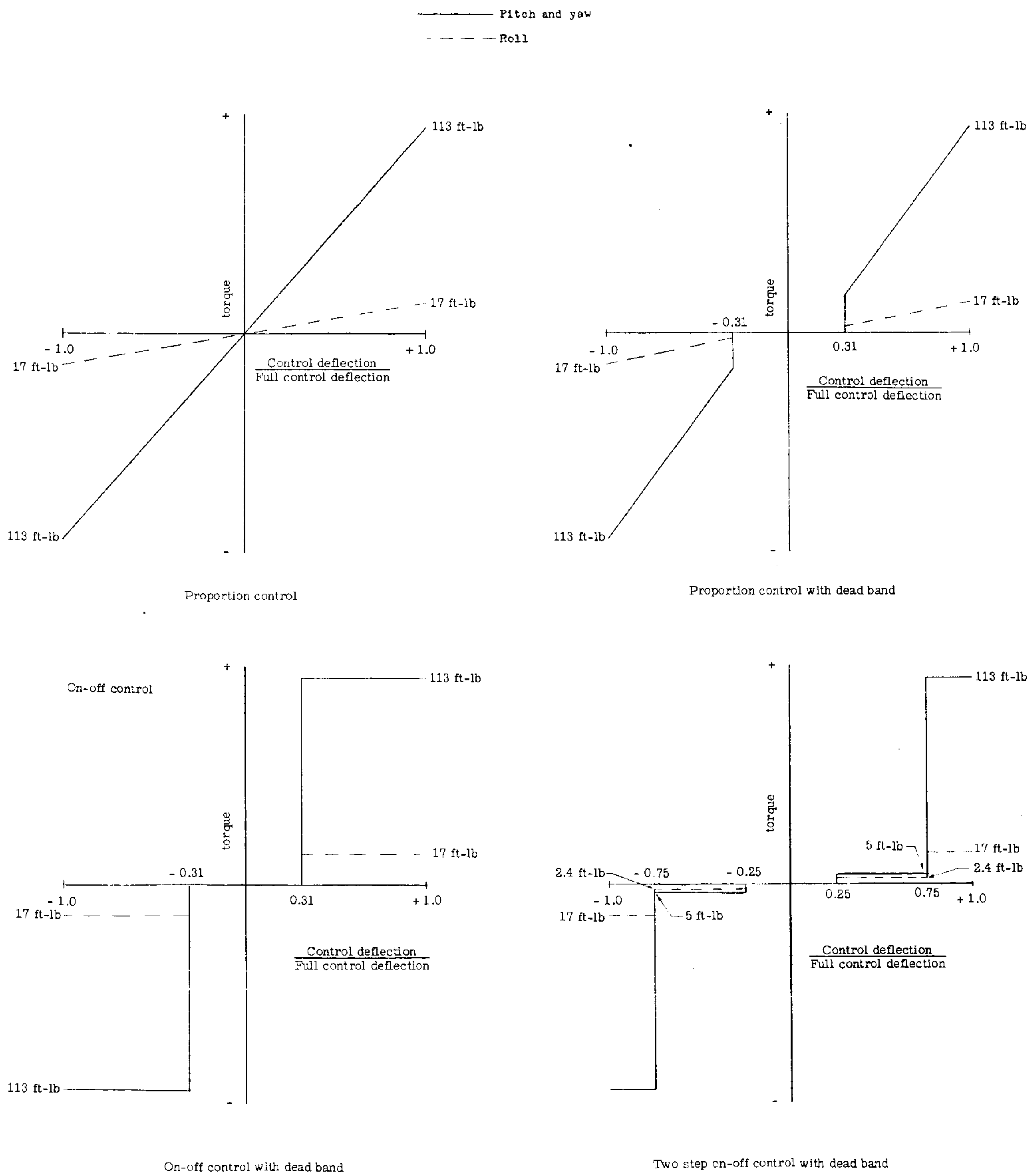

L-974

Figure 10.- Variations of control torque with controller deflection.

[redacted]

[redacted]

L-974

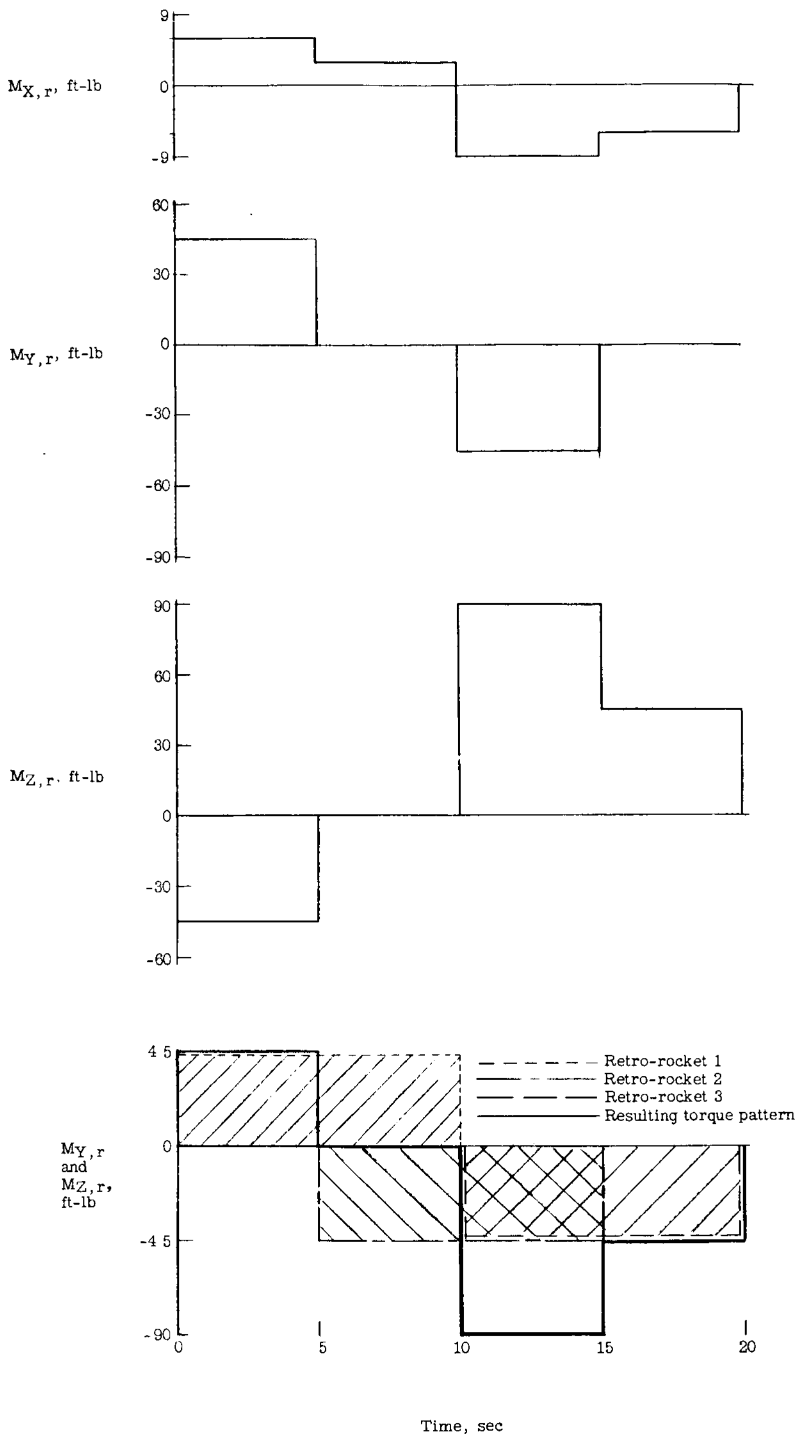

Figure 11.- Typical retro-rocket torque misalinement patterns and explanatory diagram of the origin of $M_{Y,r}$ and $M_{Z,r}$.

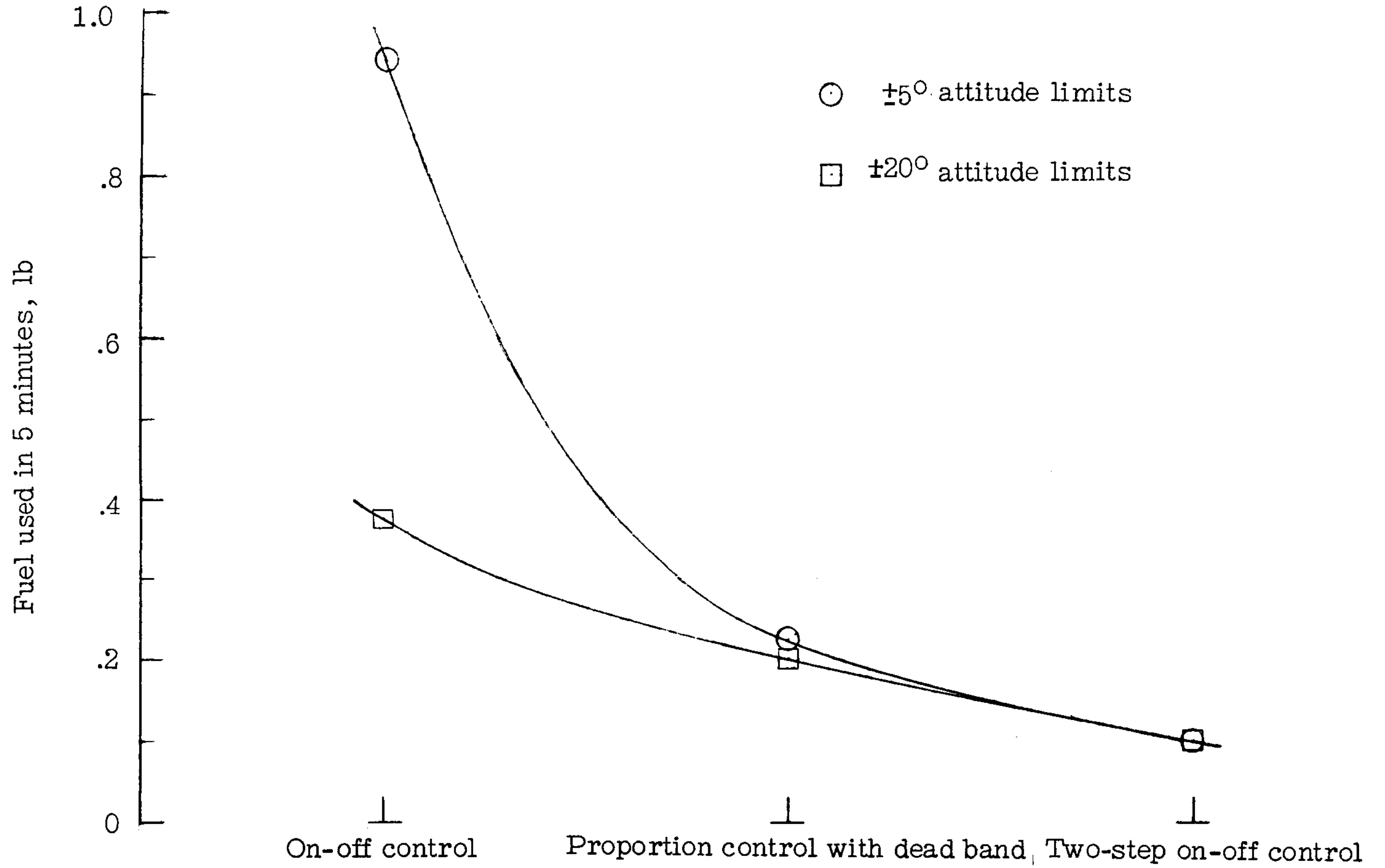

Figure 12.- Fuel expended when using three variations of control torque with deflection, for 5-minute orbital flights.

[redacted]

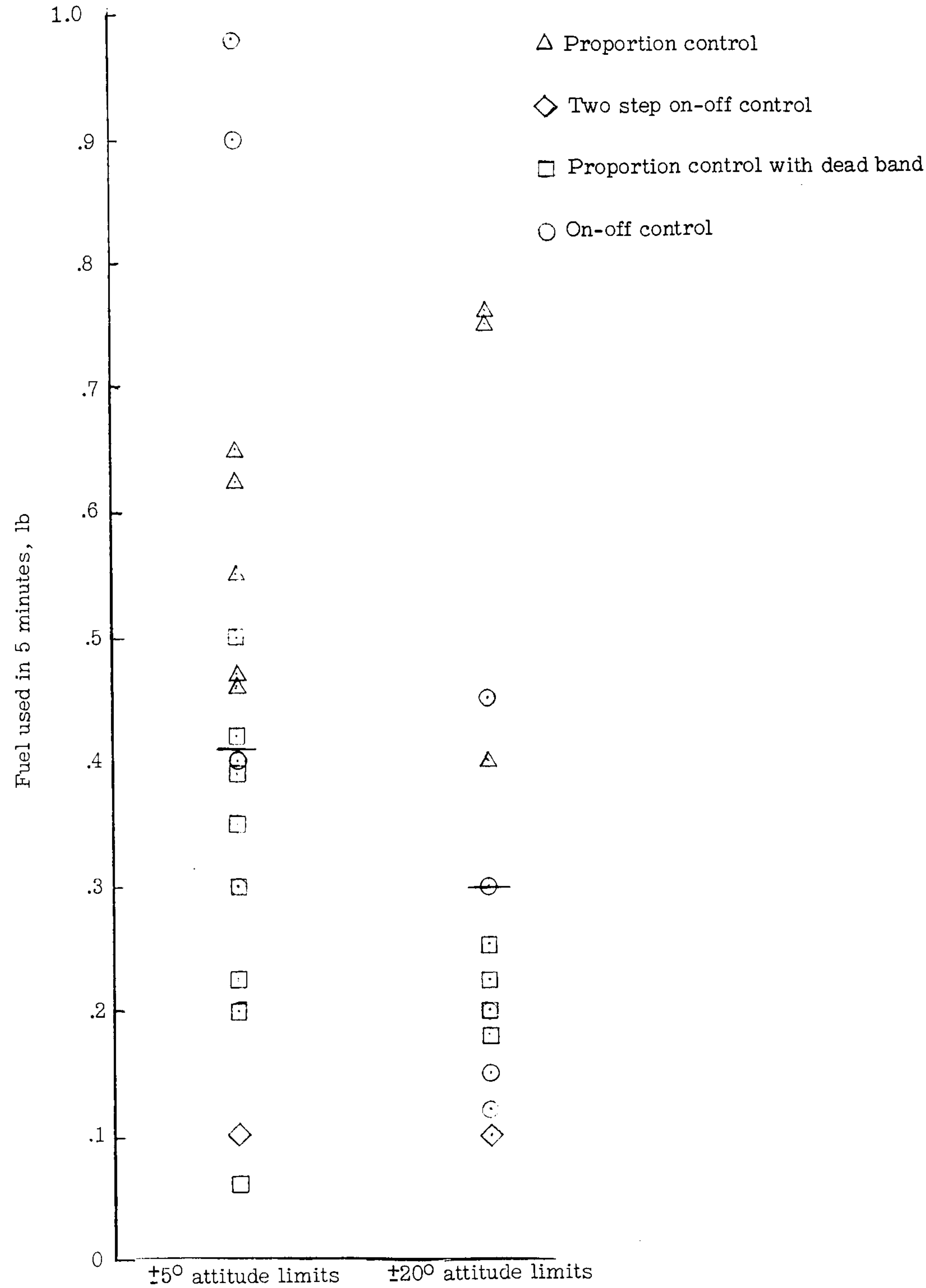

Figure 13.- Summary plot of fuel expended for 5-minute orbital flights.

L-974

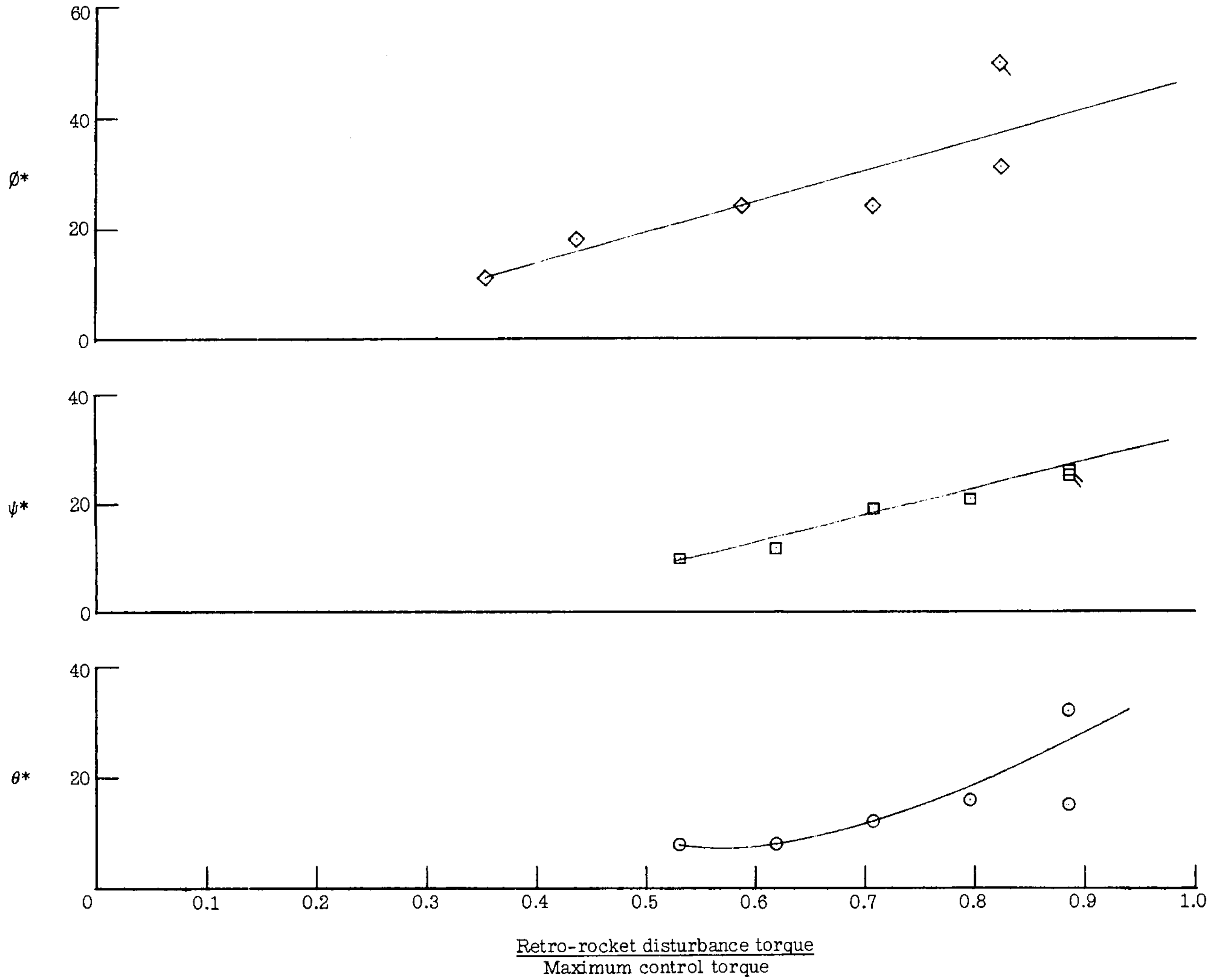

Figure 14.- Variation of attitude excursion with retro-rocket misalinement torque for a single rocket firing. Proportion control with dead band.

DECLASSIFIED [redacted]

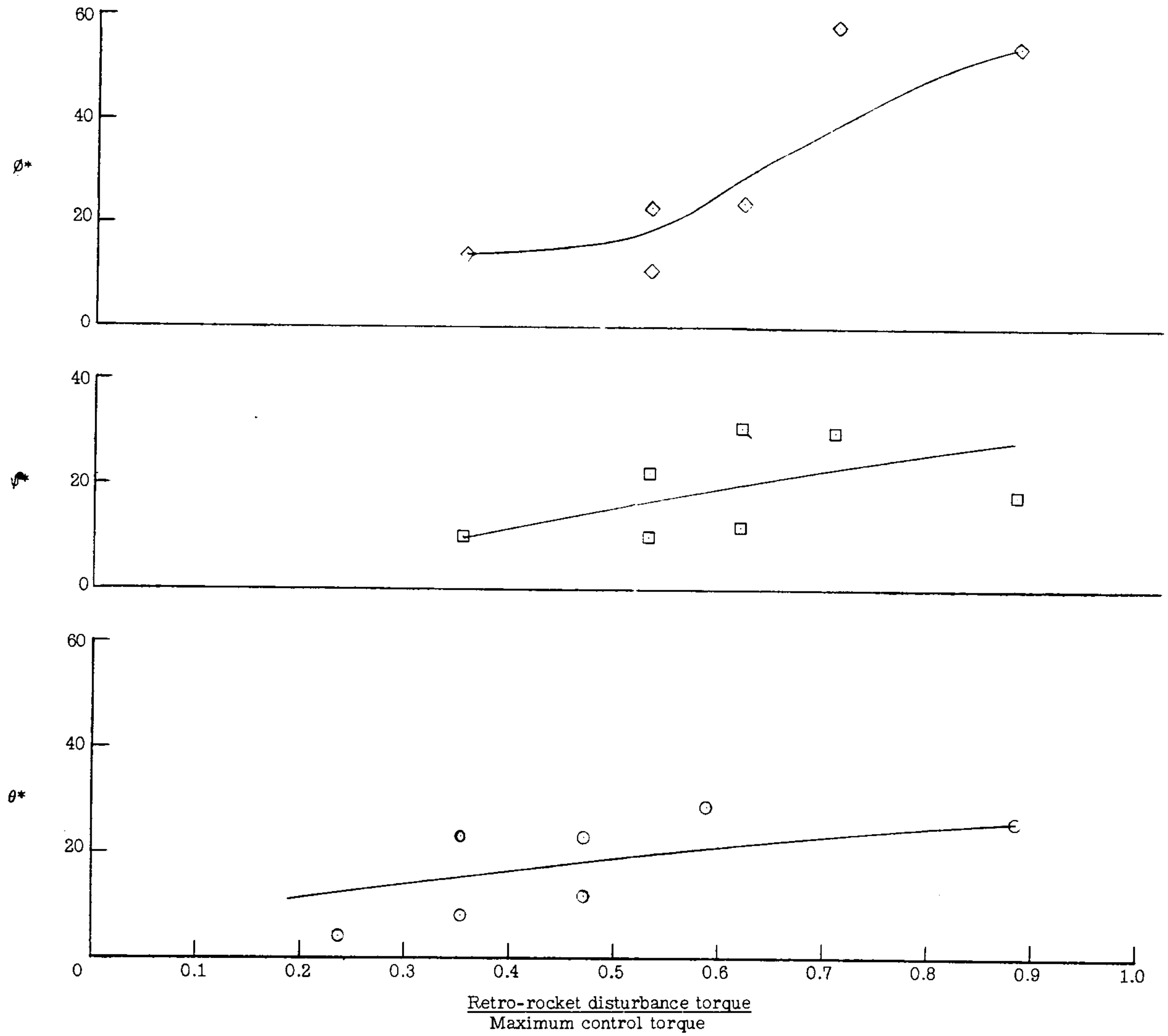

Figure 15.- Variation of attitude excursion with retro-rocket misalinement torque for a single rocket firing. On-off control.

[redacted]

V

L-974

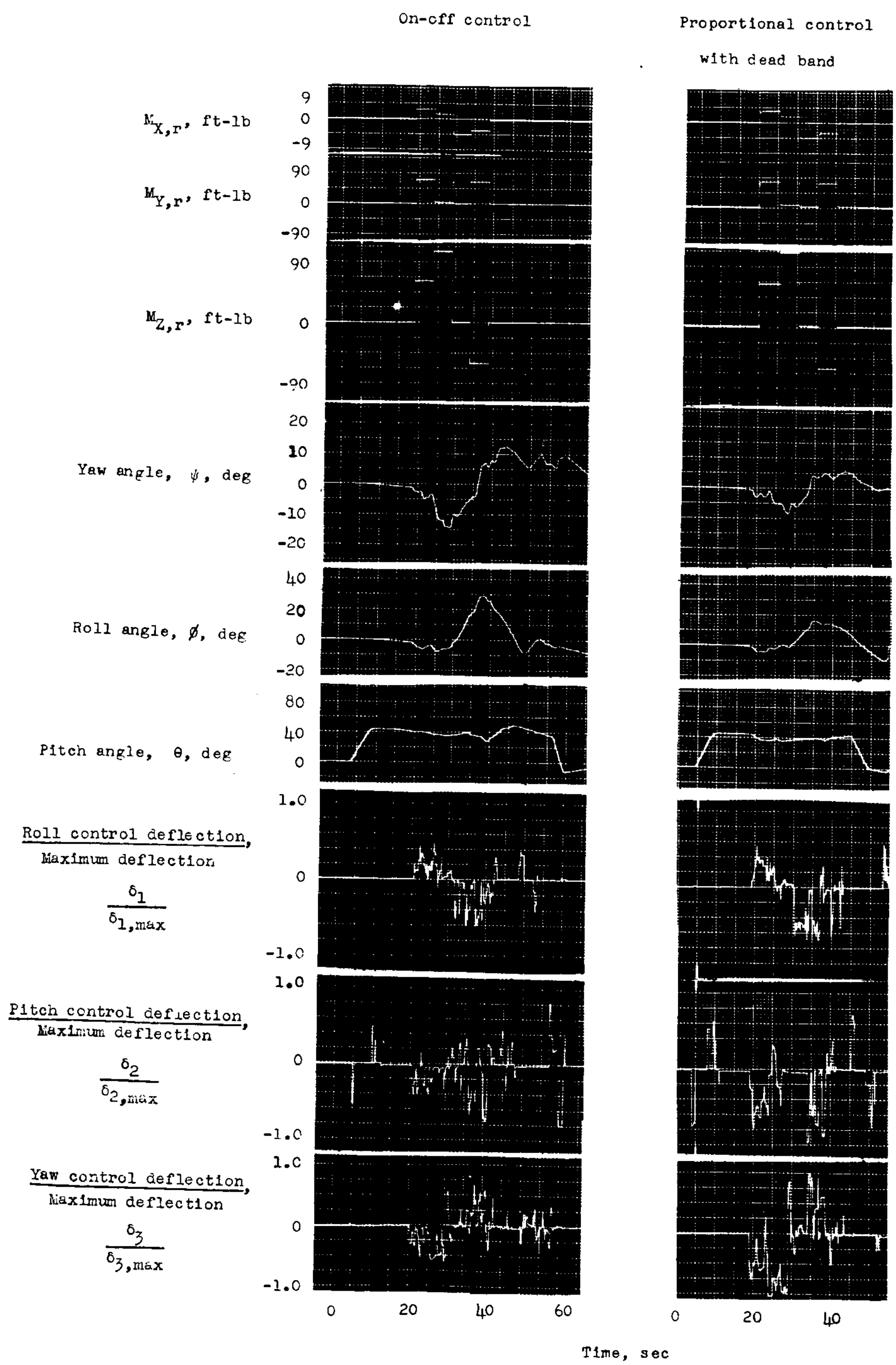

Figure 16.- Time histories of the pilot's control motions during retro-rocket firing when using the on-off control and the proportion control with dead band.

[redacted]

[redacted]

L-974

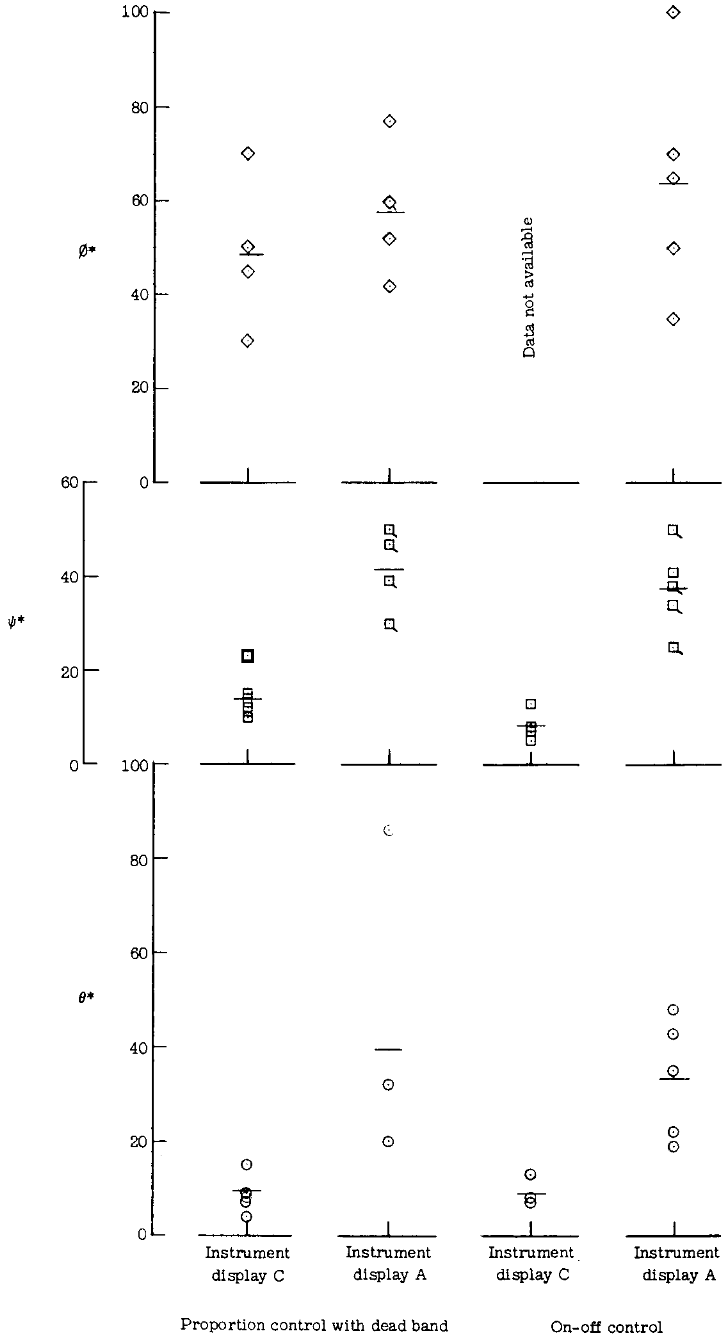

(a) Controller B.

Figure 17.- Attitude excursions compared for groups of runs made with a single controller, two instrument displays, and two control torque relations.

L-974

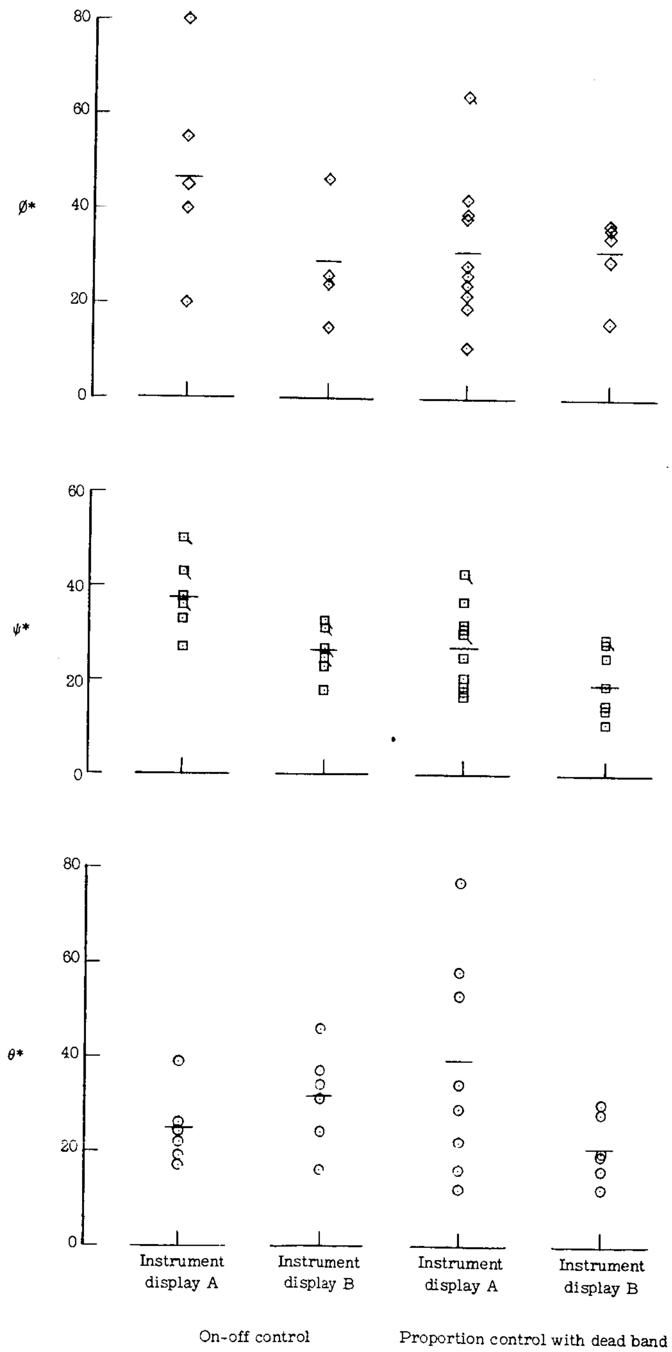

(b) Controller C.

Figure 17.- Concluded.

[redacted]

[redacted]

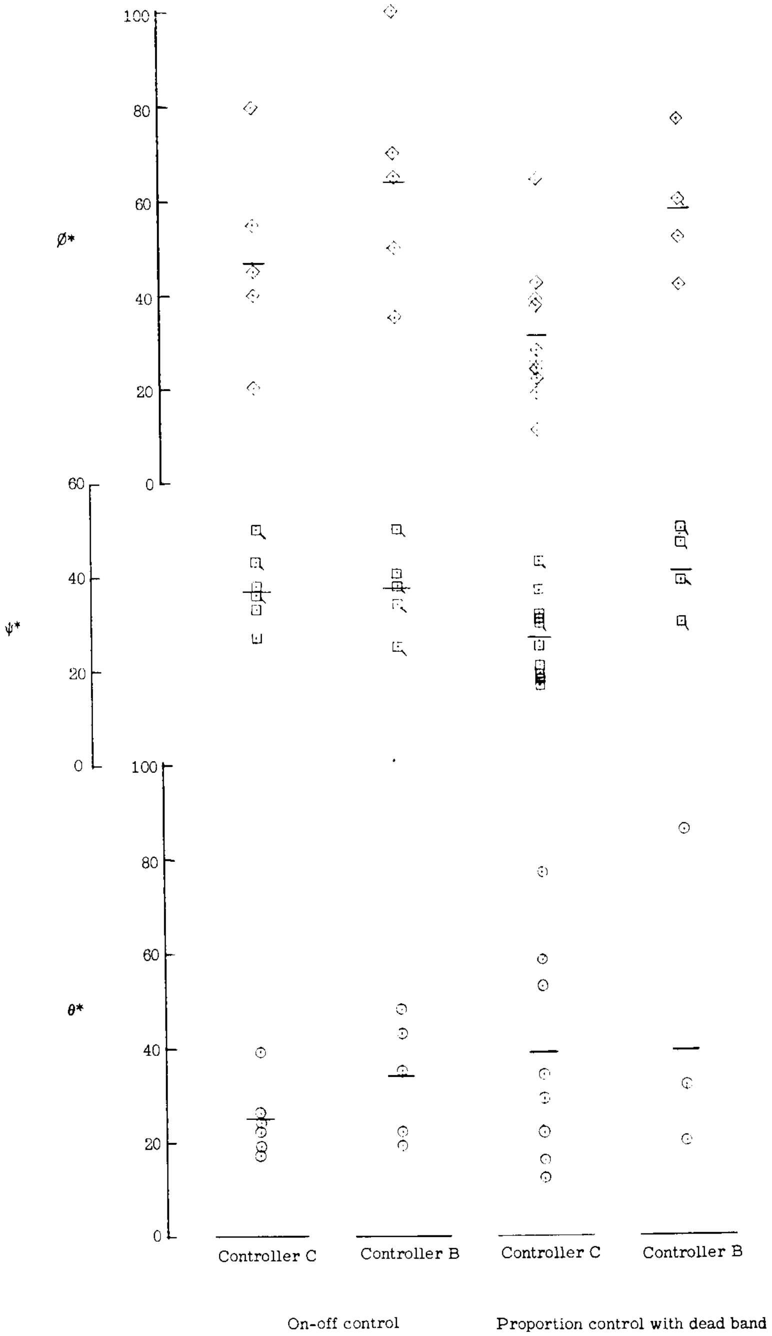

(a) Instrument display A.

Figure 18.- Attitude excursions compared for groups of runs made with a single instrument display, two controllers, and two control torque relations.

L-974

[redacted]

L-974

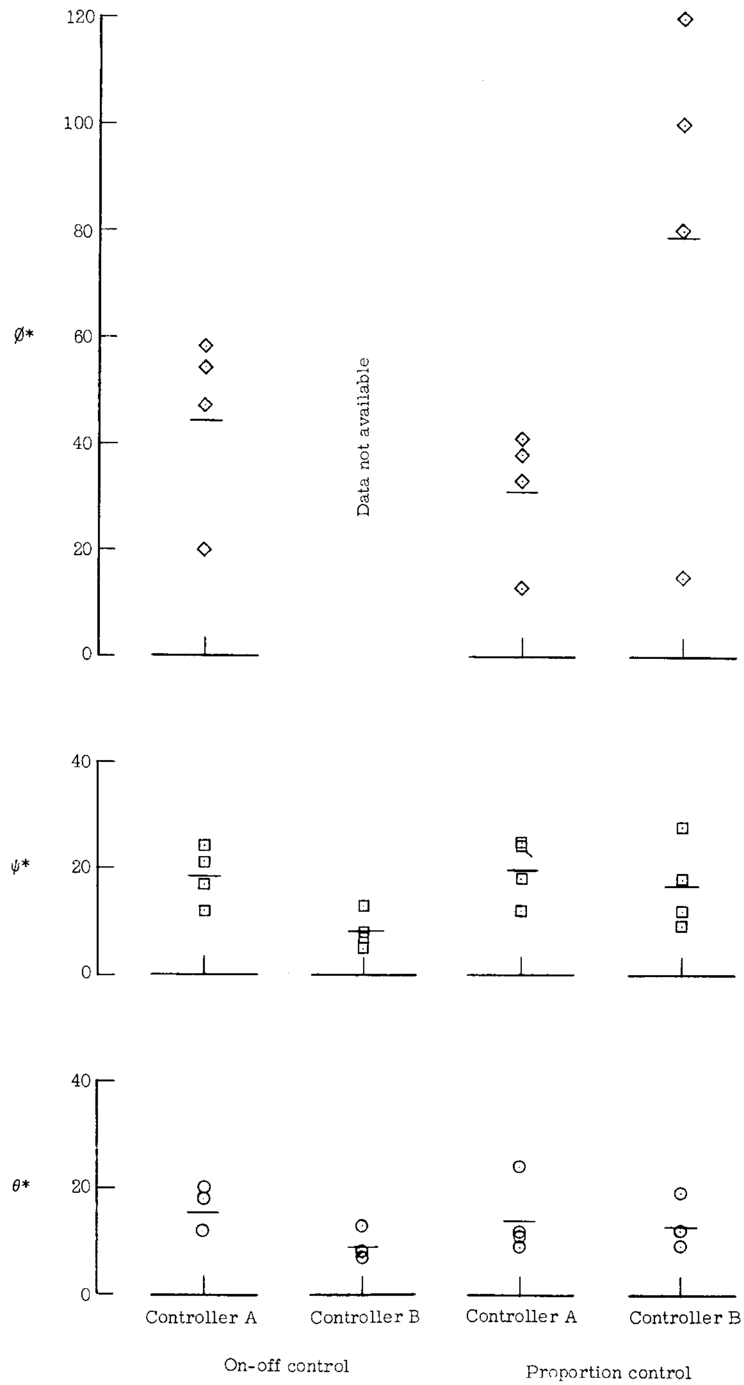

(b) Instrument display C.

Figure 18.- Concluded.

[redacted]

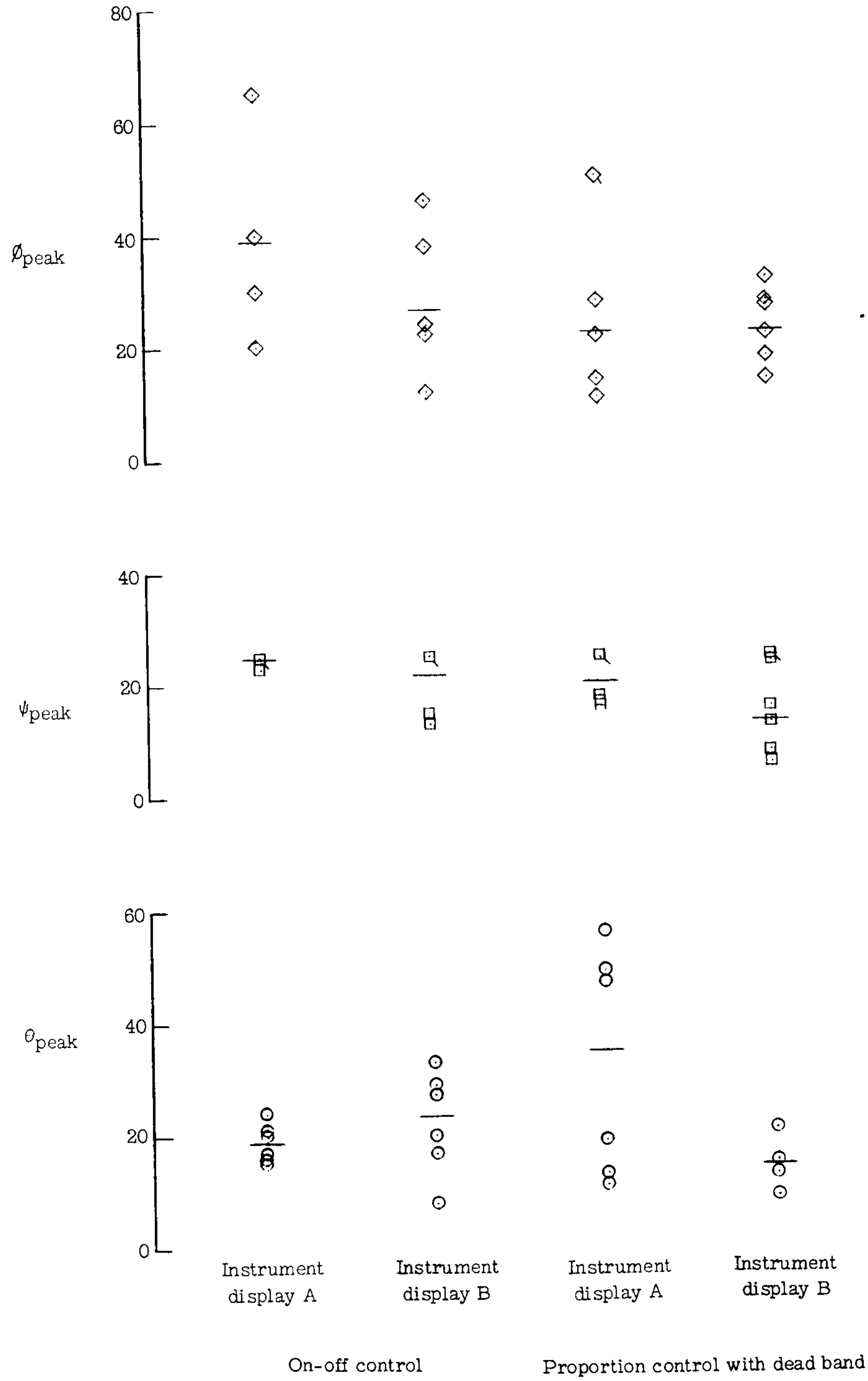

Figure 19.- Attitude peaks for the runs whose peak-to-peak excursions appear as figure 17(b). Controller C.

L-914

[redacted]

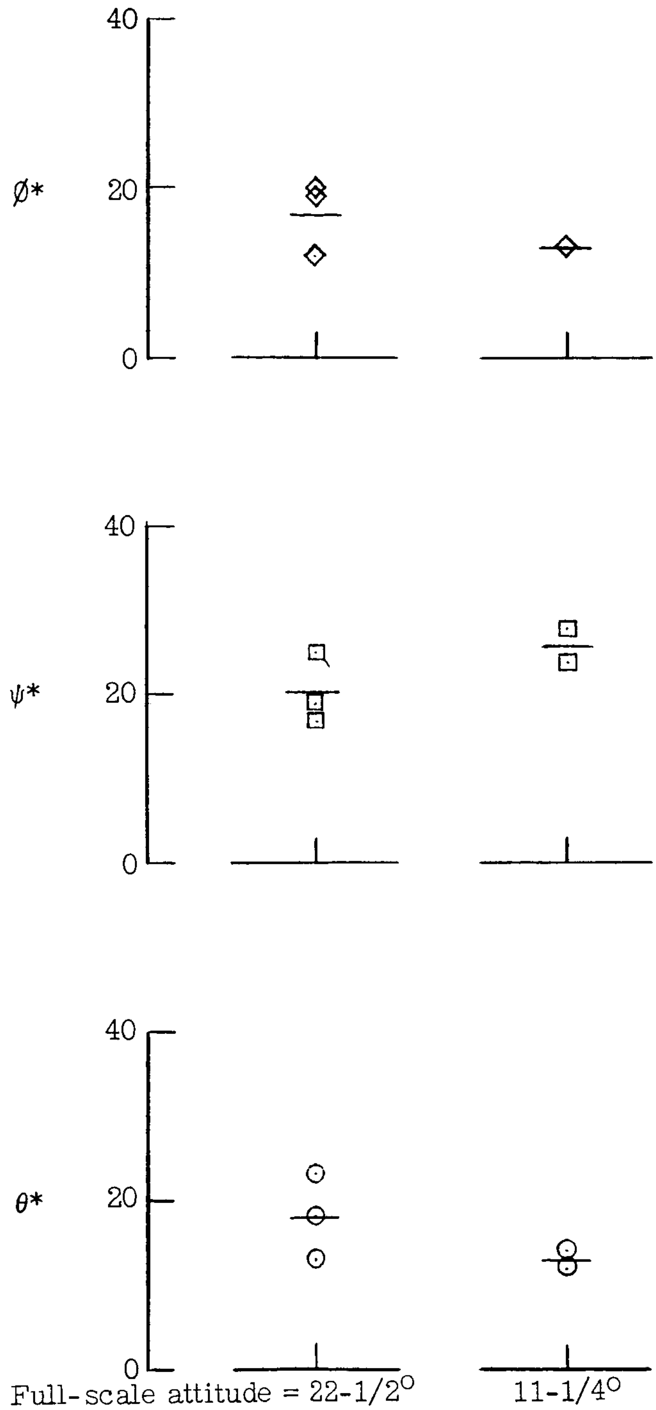

Figure 20.- Results of summing attitude and rate information on one instrument during retro-rocket firing. Proportion control with dead band; controller C.

[redacted]

[redacted]

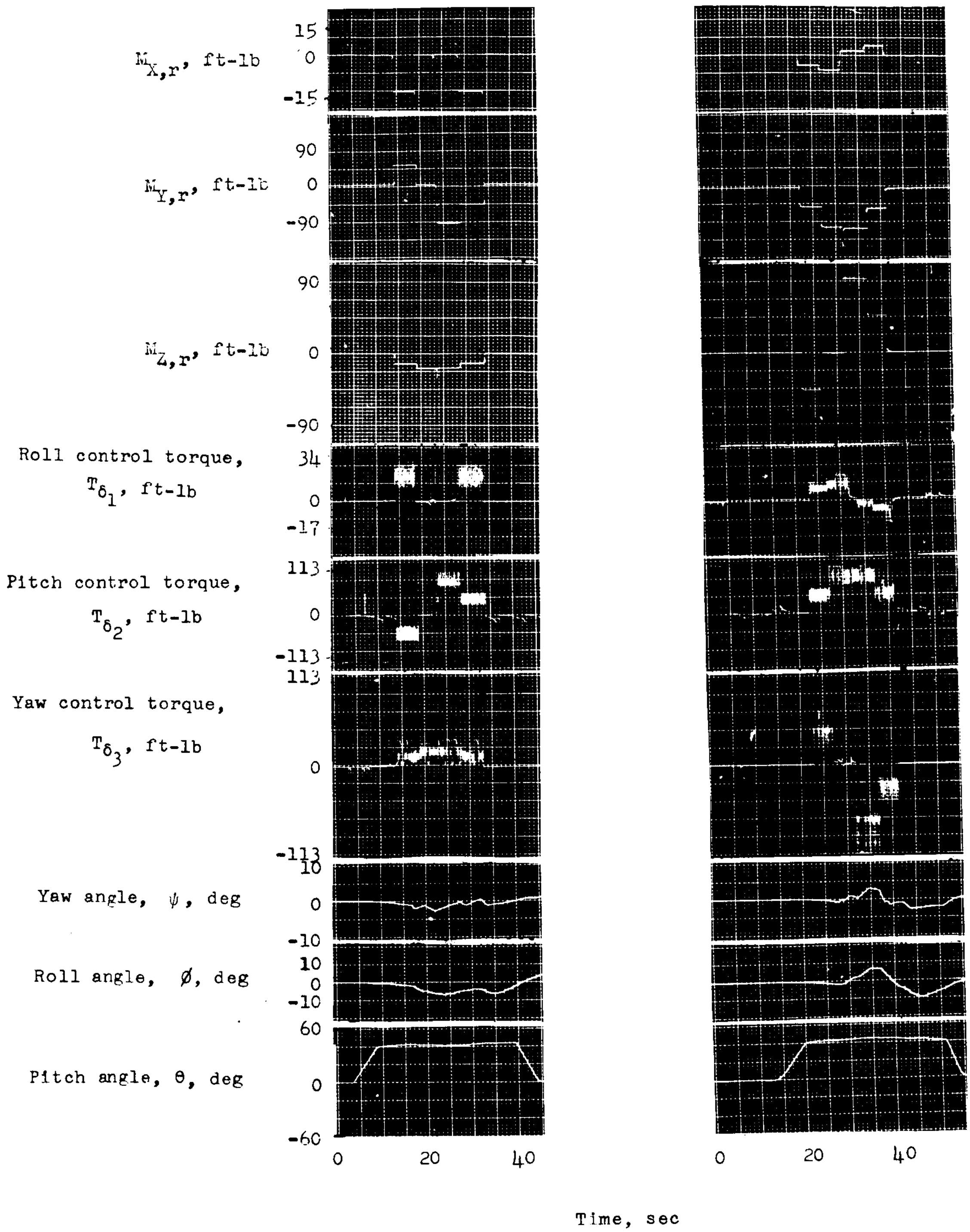

Figure 21.- Two time histories of retro-rocket firing with the rate-command control system.

[redacted]

L-974

L-974

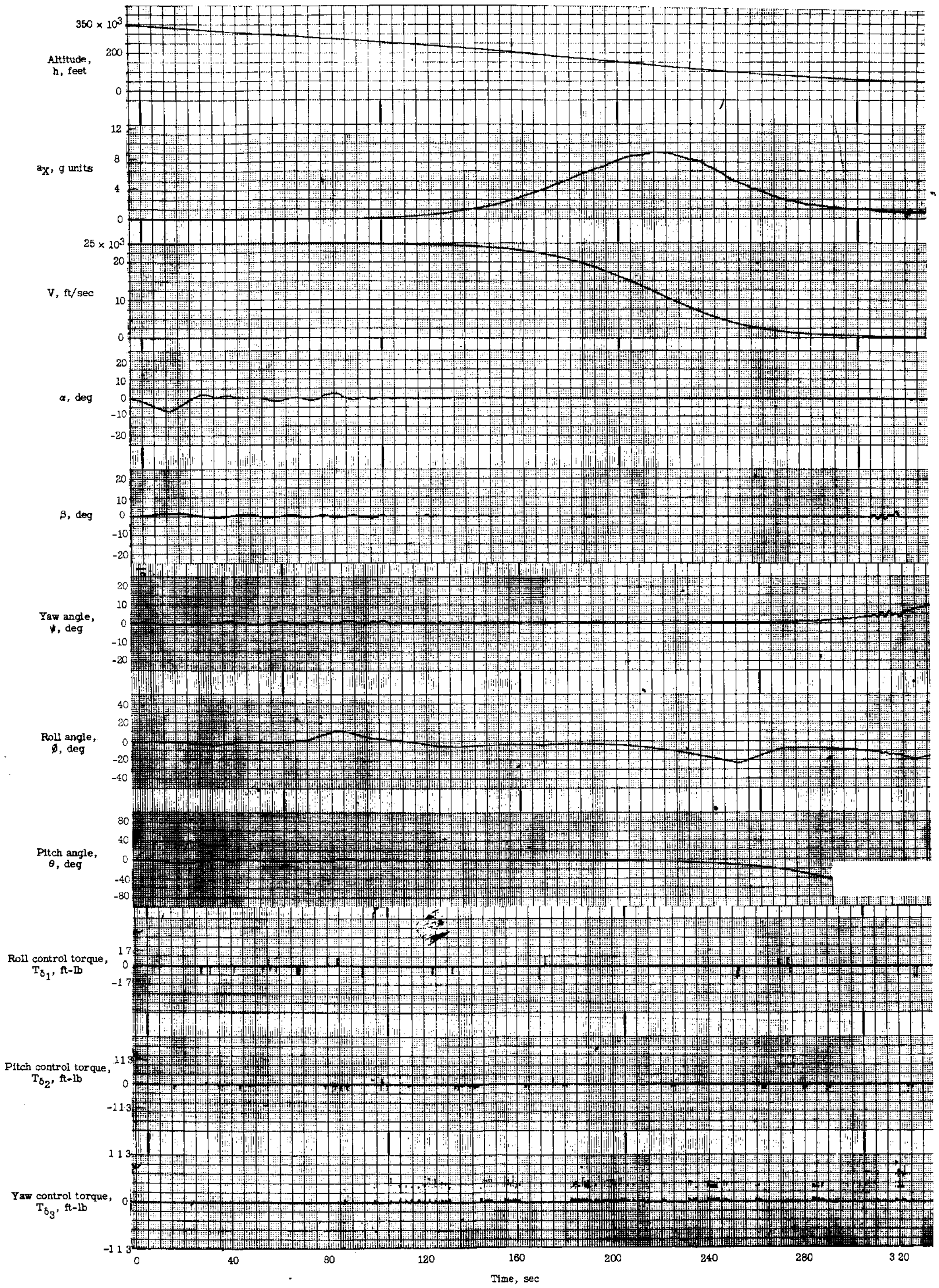

Figure 22.- Typical reentry with attitude and rate information displaye to the pilot. $\alpha_T = \beta_T = 0^\circ$.

[redacted]

L-974

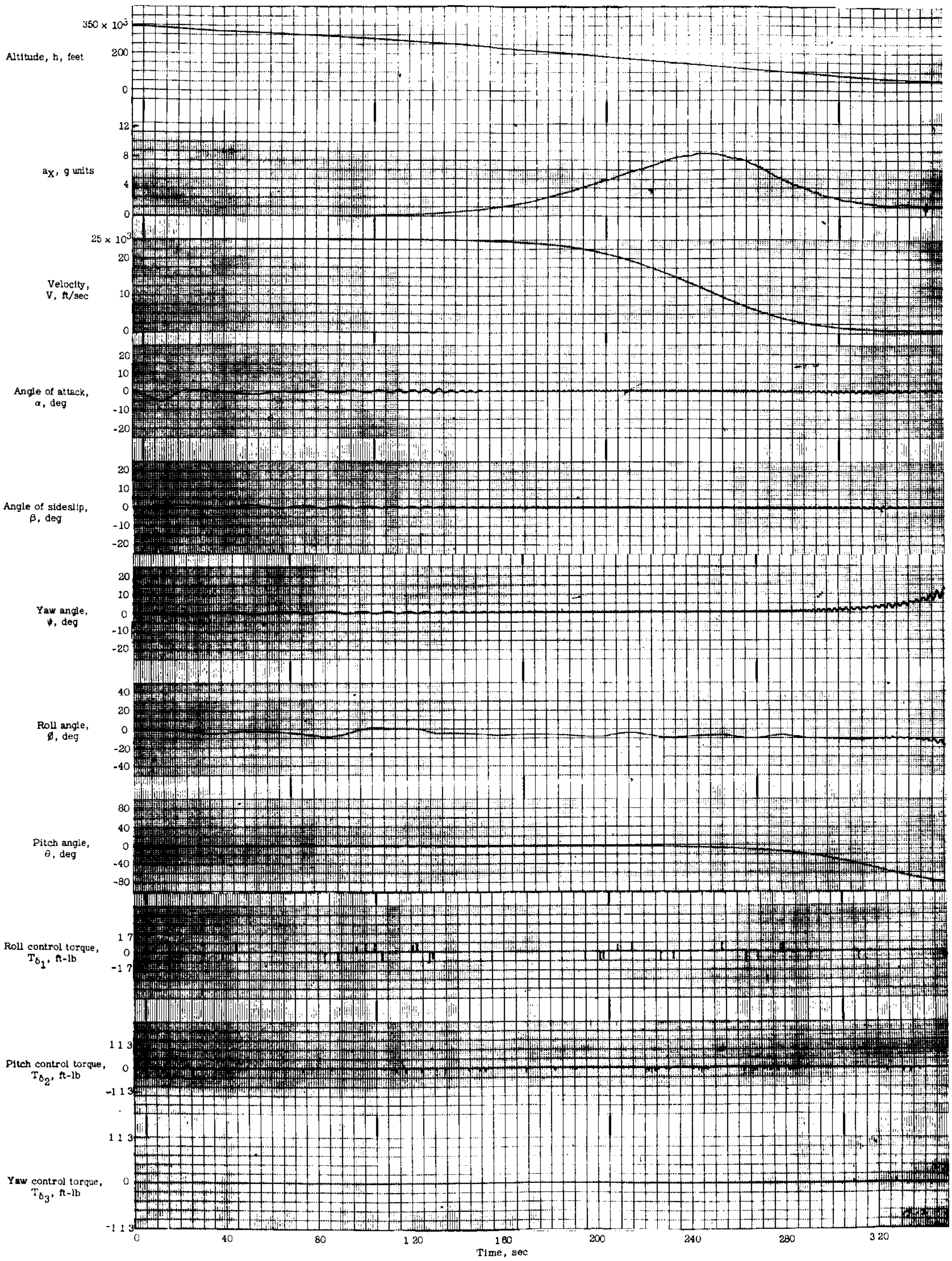

Figure 23.- Typical reentry with only attitude information displayed to the pilot. $\alpha_T = \beta_T = 0^\circ$.

[redacted]

L-974

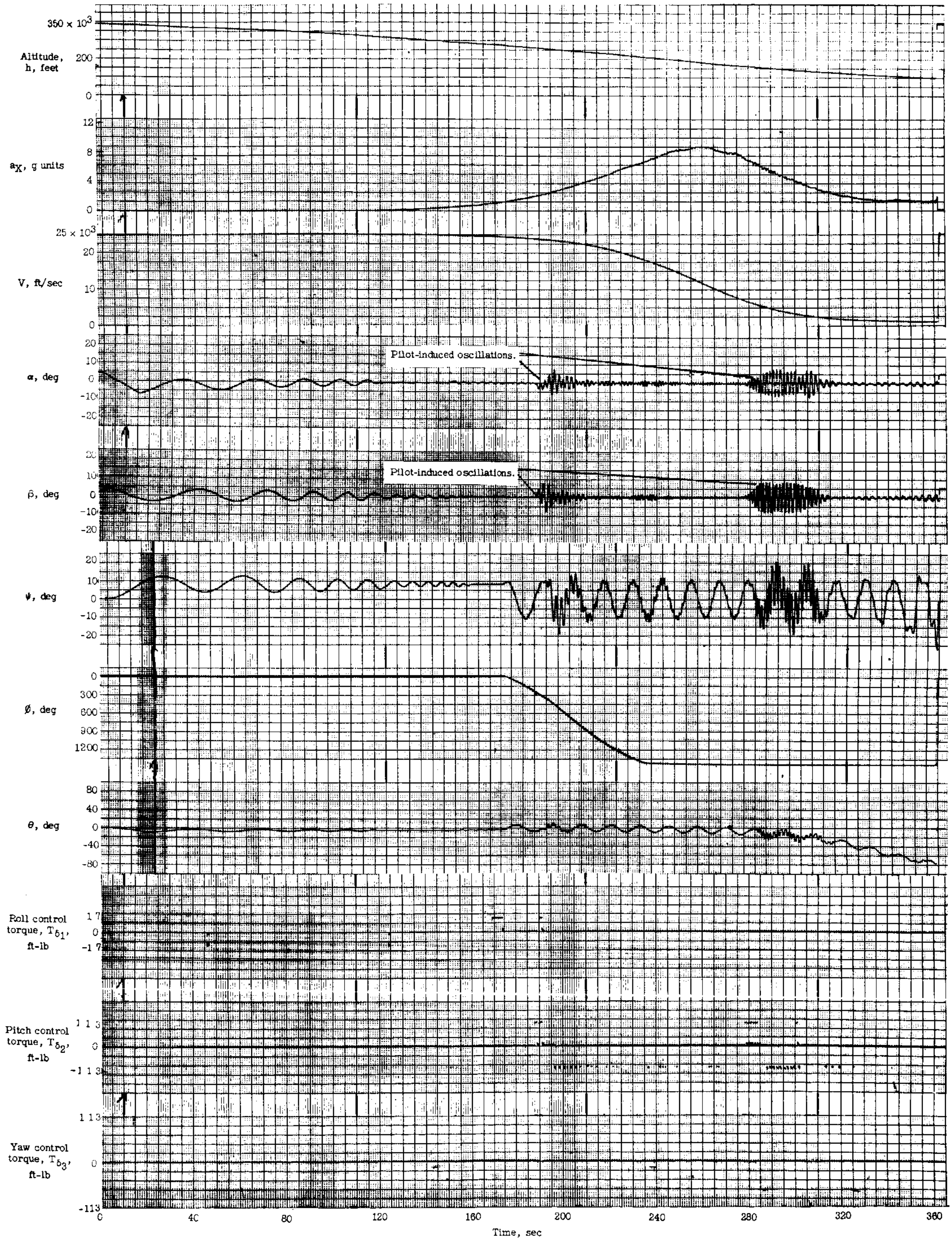

Figure 24.- Typical reentry with $\alpha_T = \beta_T = 5^{\circ}$ and constant roll rate showing deliberately excited oscillations.

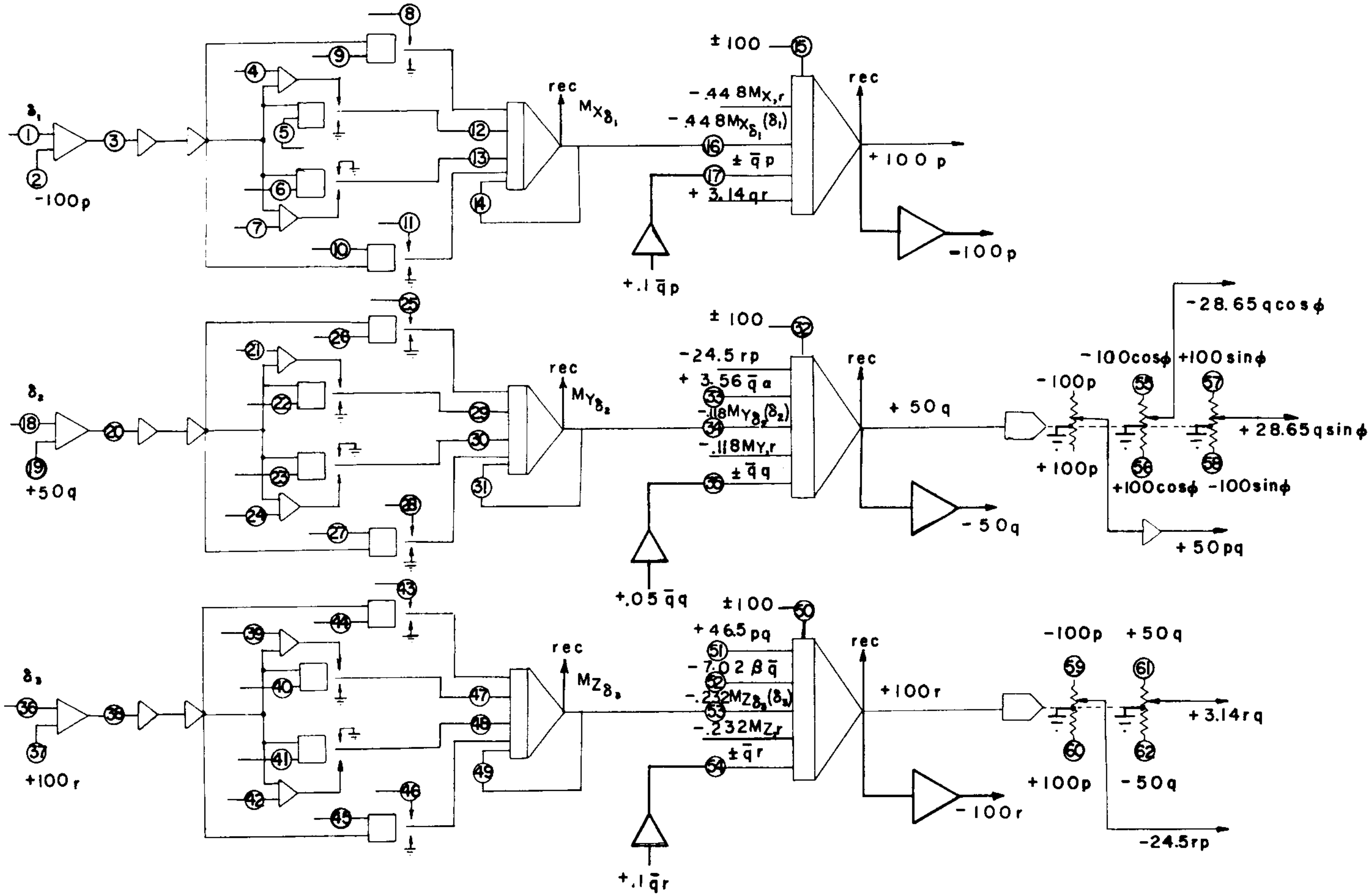

(a) Control-torque and moment-equation circuits.

Figure 25.- Schematic of analog simulation.

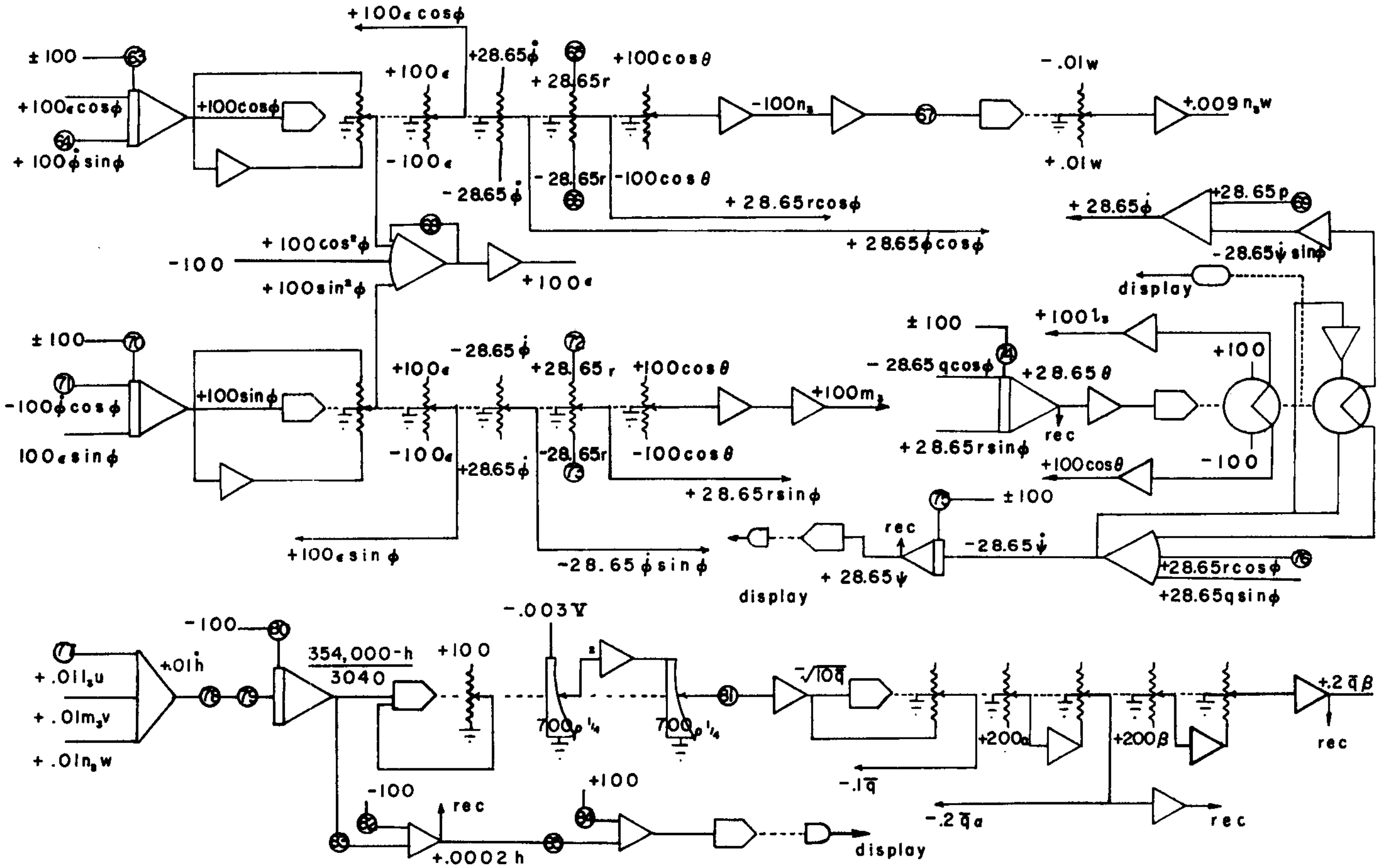

(b) Continuous-resolution, Euler angle, altitude, and dynamic-pressure circuits.

Figure 25.- Continued.

[redacted]

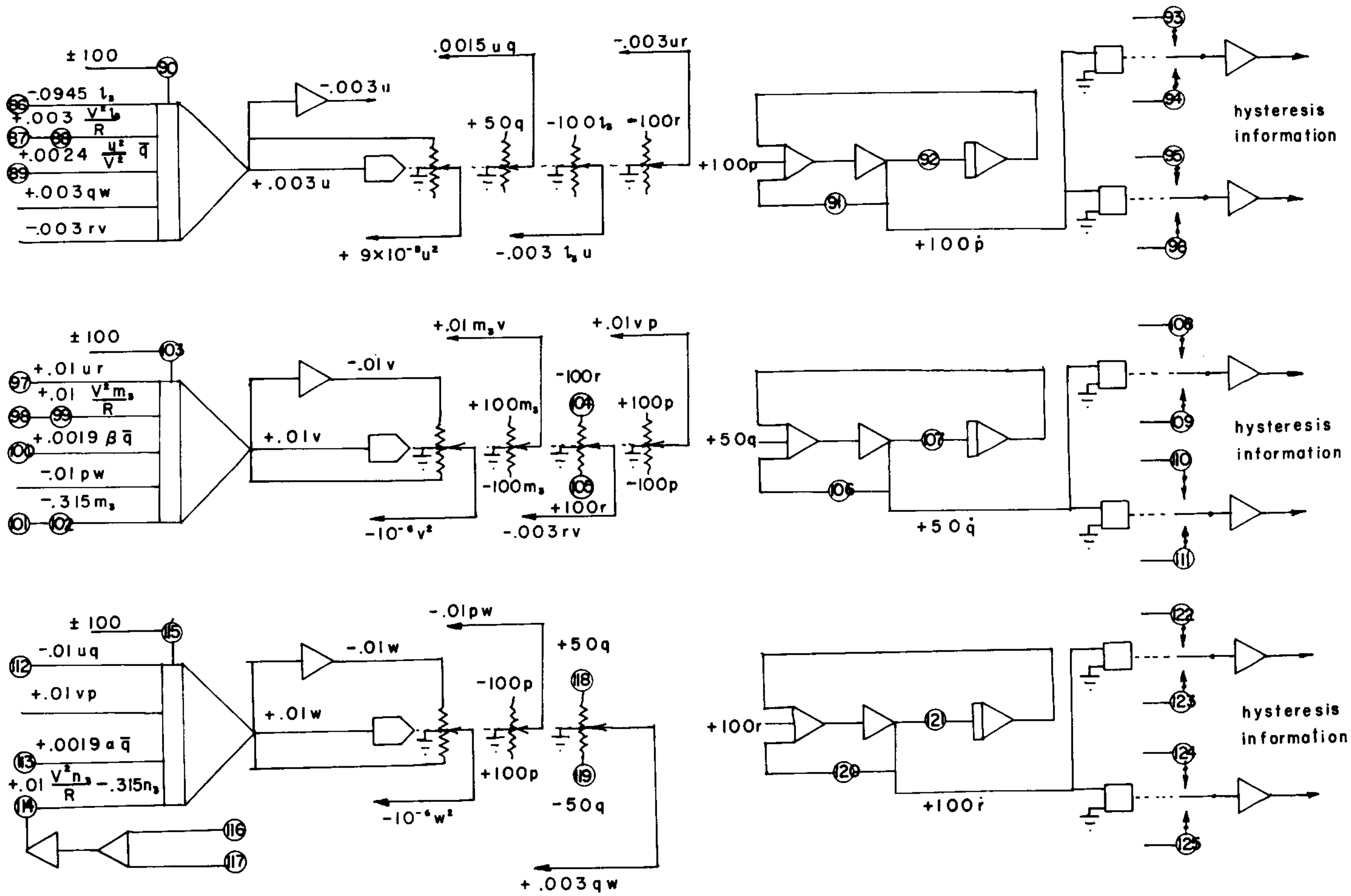

(c) Force-equation and hysteresis-information circuits.

Figure 25.- Continued.

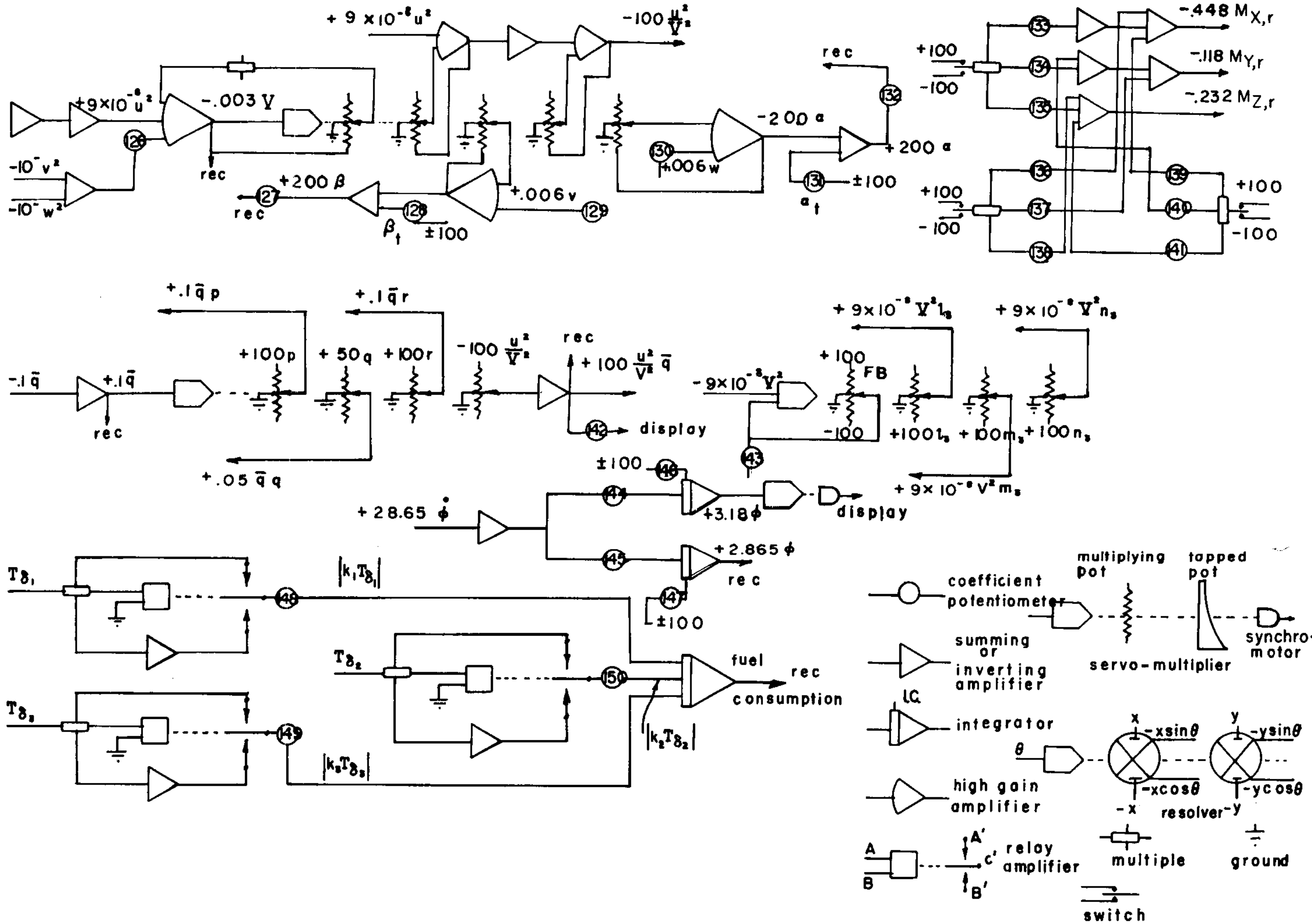

(d) Velocity, retro-rocket, and fuel-consumption circuits.

Figure 25.- Concluded.

[redacted]